

Gene Therapy

Therapeutic Mechanisms and Strategies

edited by

Nancy Smyth Templeton

*Baylor College of Medicine
Houston, Texas*

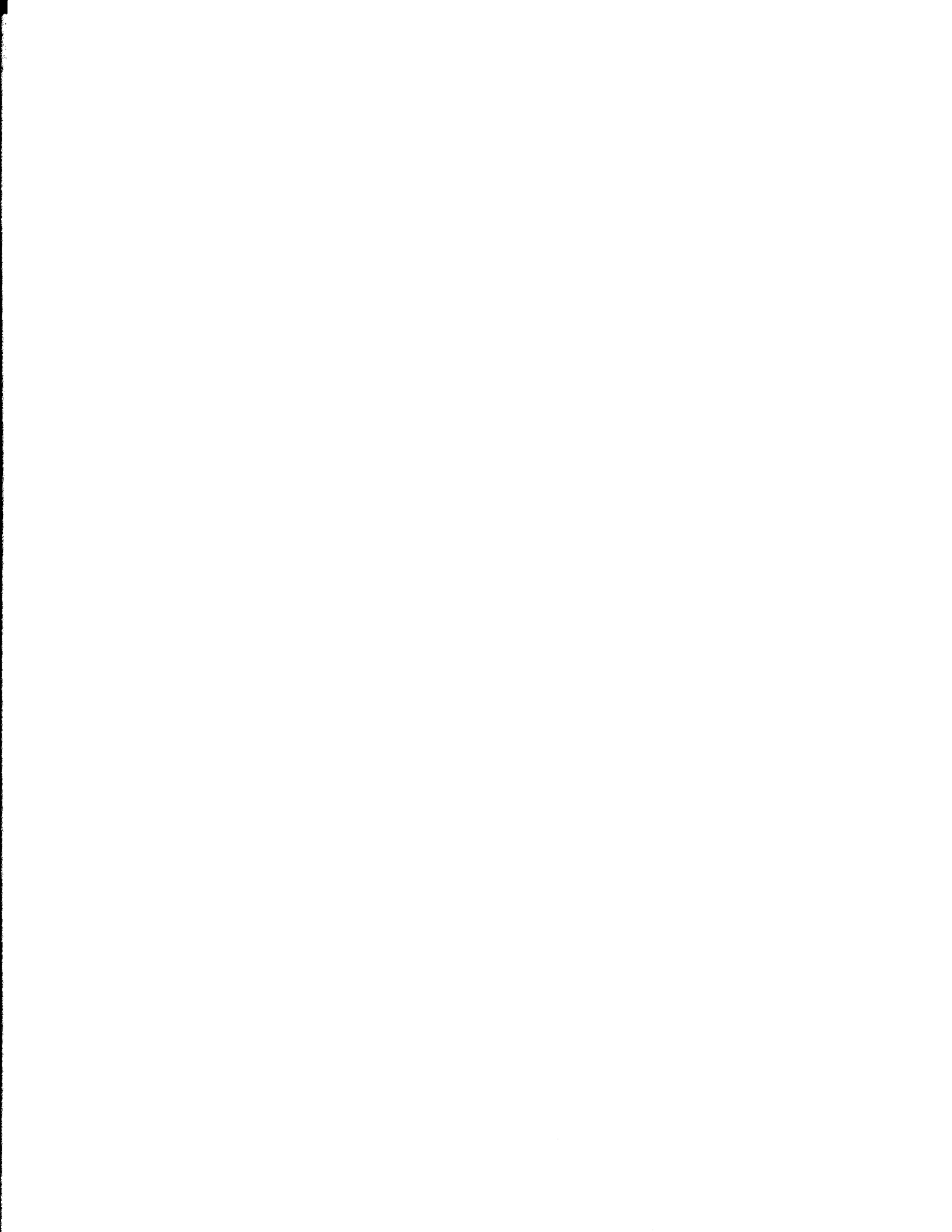
Danilo D. Lasic

*Liposome Consultations
Newark, California*



MARCEL DEKKER, INC.

NEW YORK • BASEL



Molecular Interactions in Lipids, DNA, and DNA-Lipid Complexes

Rudolf Podgornik

University of Ljubljana, Ljubljana, Slovenia, and National Institute of Child Health and Human Development, National Institutes of Health, Bethesda, Maryland

Helmut H. Strey

University of Massachusetts, Amherst, Massachusetts

V. A. Parsegian

National Institute of Child Health and Human Development, National Institutes of Health, Bethesda, Maryland

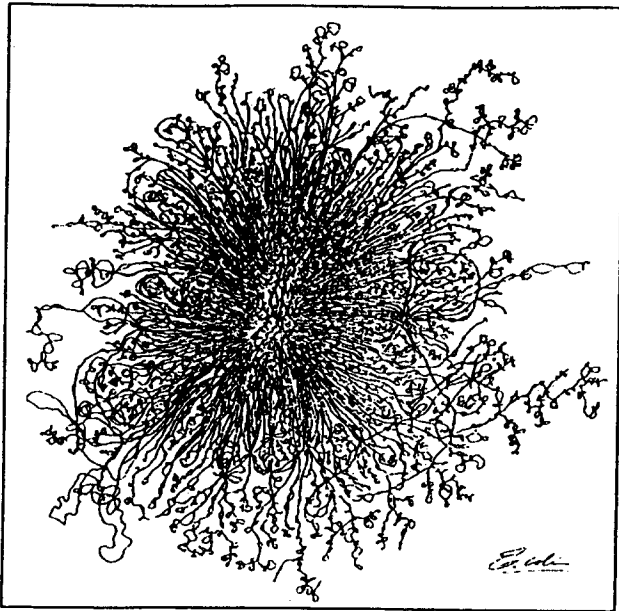
I. INTRODUCTION

Designed by nature for information, valued by molecular biologists for manipulation, DNA is also a favorite of physical chemists and physicists (1). Its mechanical properties (2), its interactions with other molecules (3), and its modes of packing (4) present tractable but challenging problems, whose answers have in vivo and in vitro consequences. In the context of DNA transfection and gene therapy (5), what has been learned about molecular mechanics, interaction, and packing might teach us how to package DNA for more effective gene transfer. Among these modes of in vitro packaging are association with proteins, treatment with natural or synthetic cationic "condensing agents," and combination with synthetic positively charged lipids (6).

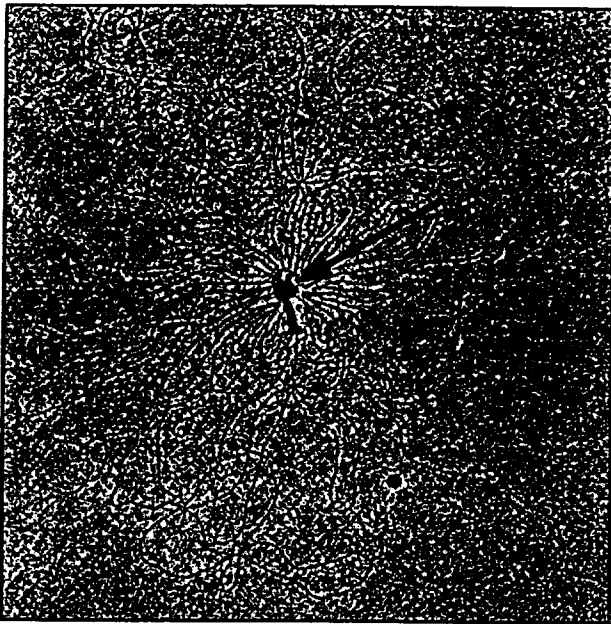
In vivo, DNA is tightly held, not at all like the dilute solution form often studied in vitro (Fig. 1). This tight assembly necessarily incurs huge energetic costs of confinement, costs that create a tension under which DNA is expected to ravel or to unravel its message. Through direct measurement of forces between DNA molecules (7) and direct observation of its modes of packing (8), we might see not only how to use concomitant energies to design better DNA-transfer systems but also to reason better about the sequences of events by which DNA is read in cells.

What binds these structures? To first approximation, for large, flexible biological macromolecules, the relevant interactions resemble those found in among colloidal particles (9), where the size of the molecule (such as DNA molecules, lipid membranes, actin bundles) distinguishes it from simpler, smaller species (such as small solutes or salt ions). On the colloidal scale of tens of nm (10^{-9} m) only the interactions between macromolecules are evaluated explicitly, while the small molecular species only "dress" the large molecules and drive the interactions between them.

The electrical charge patterns of multivalent ions such as Mn^{+2} , Co^{3+} , or spermine⁺⁴, cation binding to negative DNA, create attractive electrostatic and/or solvation forces that move DNA double helices to finite separations despite the steric knock of DNA thermal motion (10). Solvation patterns about the cation-dressed structures create solvation forces e.g., DNA-DNA repulsion because of water clinging to the surface and attraction from the release of solvent (11). Positively charged histones will spool DNA into carefully distributed skeins, themselves arrayed for systematic unraveling and reading (12). Viral capsids will encase DNA, stuffed against its own DNA-DNA electrostatic and solvation repulsion, to keep it under pressure for release upon infection (13). In artificial preparations the



Escherichia coli DNA after osmotic shock



Bacteriophage T2 DNA after osmotic shock

Figure 1 In vivo DNA is highly compacted. The figure shows *Escherichia coli* DNA and T2 bacteriophage DNA after an osmotic shock that has allowed them to expand from their in vivo configurations. (*E. coli* picture courtesy of Ruth Kavenoff, Designergenes Inc., Los Angeles, CA. T2 picture from Ref. 108. Courtesy of Elsevier Publishing Company, Oxford, England.)

glue of positively charged and neutral lipids can lump negative DNA into ordered structures that can move through lipids and through water solutions (14).

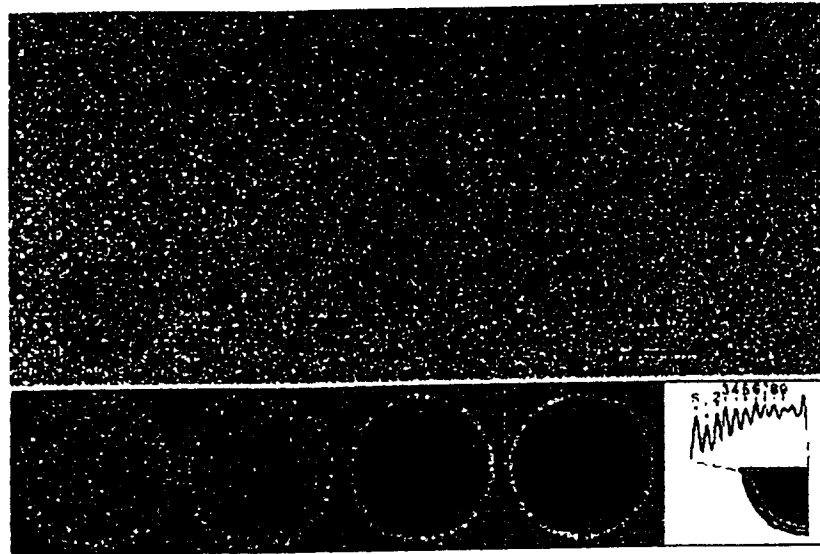
Changes in the suspending medium can modulate intermolecular forces. One example is the change in van der Waals charge fluctuation forces (see below) between lipid bilayers when small sugars modifying the dielectric dispersion properties of water are added to the solution (15). More dramatic, the addition of salt to water can substantially reduce electrostatic interactions between charged molecules such as DNA or other charged macromolecules bathed by an aqueous solution (16). These changes can modify the behavior of macromolecules quantitatively or induce qualitatively new features into their repertoire, among these most notably precipitation of DNA by addition of organic polycations to the solution (10).

Similar observations can be made about a small molecule essential to practically every aspect of interaction between macromolecules. Through the dielectric constant it enters electrostatic interactions, through pH it enters charging equilibria, and through its fundamental molecular geometry it enters the hydrogen bond network topology around simple solutes. This is, of course, the water molecule (17). In what follows we will limit ourselves to only three basic properties of macromolecules—charge, polarity (solubility), and conformational flexibility—that appear to govern the plethora of forces encountered in biology. It is no surprise that the highly ordered biological structures, such as the quasi-crystalline spooling of DNA in viral heads or the multilamellar stacking of lipid membranes in visual receptor cells, can in fact be explained through the properties of a very small number of fundamental forces acting between macromolecules (Fig. 2). Detailed experimental as well as theoretical investigations have identified hydration, electrostatic, van der Waals or dispersion, and conformational fluctuation forces as the most fundamental interactions governing the fate of biological macromolecules. Our intent here is to sketch the measurements of these operative forces and to dwell on concepts that rationalize them. It is from these concepts, with their insight into what controls organizing forces, that we expect people to learn to manipulate and to package DNA in more rewarding ways.

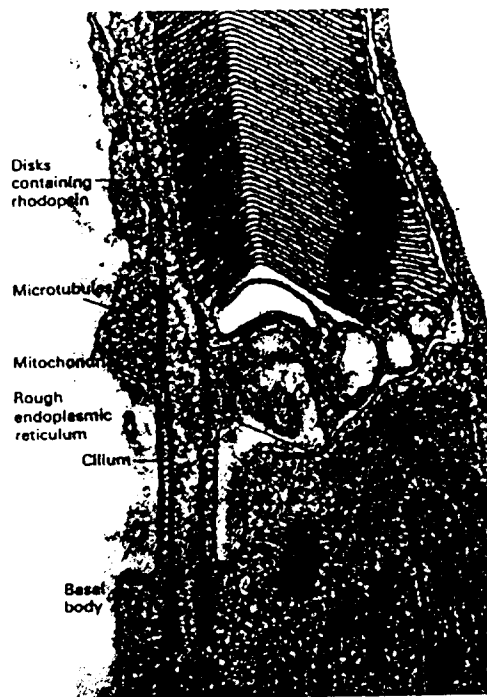
II. MOLECULAR FORCES

A. The Origin of Molecular Forces

We divide these forces into two broad categories. First, there are interactions that are connected with fields emanating from sources within or on the macromolecules them-



Cryo-micrographs and computer-processed images of T7 heads.
Bar = 50 nm.



Electron micrograph of a part of human rod cell.

Figure 2 Highly ordered assemblies, ubiquitous among biological structures, can be explained through the properties of a very small number of fundamental forces acting between macromolecules. Cryomicrographs and computer-processed images of T7 phage heads showing ordered DNA spooling within the heads (from Ref. 13). Electron micrograph of a part of a human eye rod cell. (From Ref. 109. Courtesy of Cell Press, Cambridge, MA and Harcourt Brace & Co., Orlando, FL.)

selves (16). Among these are the electrostatic fields pointing from the fixed charge distributions on macromolecules into the surrounding space; there are also the fields of connectivity of hydrogen bond networks extending from the macromolecular surfaces into the bulk solution that are seen in hydration interactions. Second are the forces due to fluctuations that originate either in thermal Brownian motion or microscopic quantum jitter (15). These interactions include the van der Waals or dispersion forces that originate from thermal as well as quantum mechanical fluctuations of electromagnetic fields in the space between and within the interacting molecules, conformation-fluctuation forces from thermal gyrations by the macromolecule when thermal agitation pushes against the elastic energy resistance of the molecule, and confinement imposed by neighboring macromolecules (16). Attraction as well as repulsion can result from either category.

B. Hydration Force

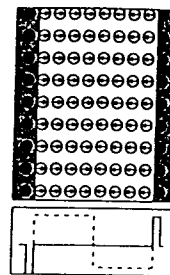
The hydration force is connected with a very simple observation that it takes increasing amounts of work to remove water from between electrically neutral lipids in multilamellar arrays or from between ordered arrays of polymers at large polymer concentrations (18). Direct measurements of this work strongly suggest that it increases exponentially with the diminishing separation between colloid surfaces, with a certain decay length that depends as much on the bulk properties of the solvent as on the detailed characteristics of the interacting surfaces.

Hydration forces can be understood in different terms with no consensus yet on mechanism (11). Marčelja and coworkers (19) first proposed the idea that colloid surfaces perturb the vicinal water and that the exponential decay of the hydration force is due to the weakening of the perturbation of the solvent as a function of the distance between the interacting surfaces. They introduced an order parameter, P , as a function of the spatial coordinates between the surfaces, $P(r)$, that would capture the local condition or local ordering of solvent molecules between the surfaces. The detailed physical nature of this order parameter is left unspecified, but since the theory builds on general principles of symmetry and perturbation expansions, molecular details are not needed. All one needs to know about P is that within the bulk water $P = 0$ and close to a macromolecular surface P remains nonzero. As a mnemonic device, one can envision P as an arrow associated with each water molecule. In the bulk the arrows point in all directions with equal probability. Close to a bounding macromolecular surface, they point preferentially towards or away from the surface (Fig. 3).

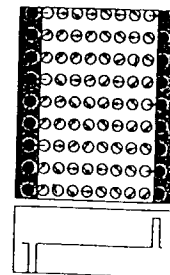
If we envisage solvent molecules between two perturbing surfaces we can decompose the total free energy

$$F = W - TS$$

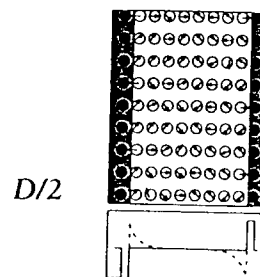
Energy minimization:



Entropy minimization:



Free energy minimization:



$$F = \frac{1}{2} a \int_{(V)} d^3 r (\nabla P(r))^2 + \frac{1}{2} b \int_{(V)} d^3 r P^2(r)$$

$$P(-D/2) = -P(D/2)$$

Figure 3 The theory of hydration force. Marčelja and Radić (19) introduced an order parameter P that would capture the local condition, or local ordering, of solvent molecules between the surfaces. We represent it as a vector on each water molecule that is trapped between the two opposing surfaces. The detailed physical nature of this order parameter is left unspecified, but because the theory builds on general principles of symmetry and perturbation expansion, molecular details are not needed. Energy minimization leads to ordering of P at the two surfaces, whereas entropy favors completely disordered configurations. Free energy minimization leads to a nonmonotonic order parameter profile. For formalism, see main text.

into its energy and entropy parts. Energetically it would be most favorable for the surface-induced order to persist away from the surfaces, but that would create conflict between the opposing surfaces (see Fig. 3). Entropy fights any type of ordering and wants to eliminate all orderly configurations between the two surfaces, creating a homogeneous state of molecular disorder characterized by $P = 0$. Energy and entropy compromise to create a nonuniform profile of the order parameter between the surfaces; surface-induced order propagates but progressively decreases away from the surfaces.

Formalizing this qualitative discussion, we can decompose the total free energy due to the order parameter variations as

$$F = \frac{1}{2}a \int_{(v)} dV (\nabla P)^2 + \frac{1}{2}b \int_{(v)} dV P^2$$

where the first term stems from the entropic cost to create inhomogeneous order parameter distributions, $\text{div } P(r) \neq 0$, while the second one originates in the energy, preferring configurations with no net order parameter, i.e., $P(r) = 0$.

Minimizing this free energy *ansatz* with respect to all order parameter profiles and taking into account that for two equal surfaces their order parameters should describe ordering that points in opposite directions, one has to assume first of all that the vectorial order parameter has only one component that depends only on the transverse coordinate, $P(r) = P(z)$, as well as that $P(z = D/2) = -P(z = -D/2)$. Clearly the total separation between the surface is D . Solving now this mathematically well-defined problem, we end up with the following form of the free energy

$$F(D) = \frac{1}{2} \frac{P(D/2)^2}{a} \sinh^{-2}(D/2\lambda_H)$$

which decays approximately exponentially with D , with a decay length of $\lambda_H = (a/b)$. Measured decay lengths are usually within the range of 0.5–3 Å. Osmotic pressure between two apposed lipid surfaces has been measured extensively for different lipids (20). From these experiments one can deduce the ratio of $P^2(D/2)$ to $(a \lambda_H)$, which for a great variety of lipids and lipid mixtures can be found within an interval of 10^{12} – 10^{10} dynes/cm². From this simple theory, the hydration force should decay with a universal decay length, depending only on the bulk properties of the solvent, i.e., the constants a and b .

In order to generalize this simplification, Kornyshev and Leikin (21) formulated a variant of the hydration force theory to take into account explicitly also the nature of surface ordering. They derive a modified decay length that clearly shows how the surface order couples with the hydration force decay length. Without going too deeply into this theory, we note that if the interacting surfaces have two-dimensional ordering patterns characterized by a wave vector $Q = 2\pi/\lambda$, where λ is their characteristic scale, then the hydration force decay length should be

$$\lambda_{KL} = \frac{1}{2\sqrt{Q^2 + \lambda_H^{-2}}}$$

Given the experimentally determined variety of forces between phospholipids (20), it is indeed quite possible that even in the simplest cases the measured decay distances are not those of the water solvent itself.

The other important facet of this theory is that it predicts that in certain circumstances the hydration forces can be-

come attractive (11). This is particularly important in the case of interacting DNA molecules, where this hydration attraction connected with condensing agents can hold DNAs into an ordered array even though the van der Waals forces themselves would be unable to accomplish that (22). This attraction is always an outcome of nonhomogeneous surface ordering and arises in situations where apposing surfaces have complementary checkerboard-like order (11). Unfortunately, in this situation many mechanisms can contribute to attractions; it is difficult to argue for one strongest contribution.

C. Electrostatic Forces

Electrostatic forces between charged colloid bodies are among the key components of the force equilibria in (bio)colloid systems (23). At larger separations they are the only forces that can counteract van der Waals attractions and thus stabilize colloid assembly. The crucial role of the electrostatic interactions in (bio)colloid systems is well documented and explored following the seminal realization of Bernal and Fankuchen (24) that electrostatic interaction is the stabilizing force in TMV arrays.

Although the salient features of electrostatic interactions of fixed charges in a sea of mobile countercharges and salt ions are intuitively straightforward to understand, they are difficult to evaluate. These difficulties are clearly displayed by the early ambiguities in the sign of electrostatic interactions between two equally charged bodies that was first claimed to be attractive (Levine), then repulsive (Verwey-Overbeek), and finally realized to be usually repulsive except if the counterions or the salt ions are of higher valency (25).

Here we introduce the electrostatic interaction on an intuitive footing (Fig. 4). Assume we have two equally charged bodies with counterions in between. Clearly the minimum of electrostatic energy W (28) for the electrostatic field configuration $E(r)$ is as follows (in MKS units):

$$W = \frac{1}{2}\epsilon\epsilon_0 \int E^2(r)dV$$

where the integration extends over all the volume with a nonzero electrostatic field, which would correspond to adsorption of counterions to the charges leading to their complete neutralization. However, at finite temperatures it is not the electrostatic energy but rather the free energy, $F = W - TS$, containing the entropy of the counterion distribution that should be minimized (26). The entropy of the mobile particles with the local density $\rho_i(r)$ (we assume there are more than one species of mobile particles, e.g., counterions and salt ions, tracked through the index, i) is taken as an ideal gas entropy (26),

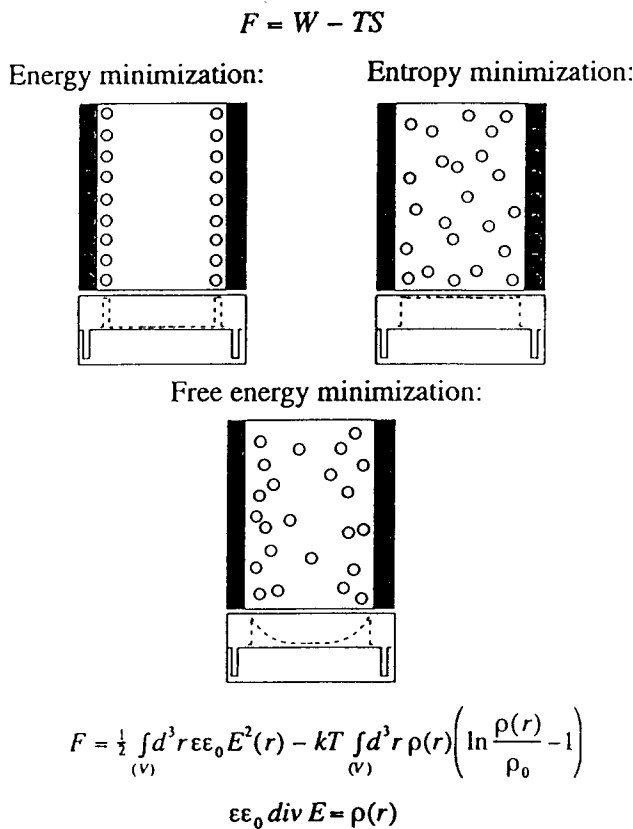


Figure 4 A pictorial exposition of the main ideas behind the Poisson-Boltzmann theory of electrostatic interactions between (bio)colloids. Electrostatic energy by itself would favor adsorption of counterions (white circles) to the oppositely charged surfaces (black circles), to the contrary, to the contrary, a completely disordered configuration, a uniform distribution of counterions between the surfaces. The free energy works a compromise between the two principles leading to a nonmonotonic profile of the counterion density (25). As the two surfaces are brought close, the overlapping counterion distributions create repulsive forces between them.

$$S = k \int \sum_i (\rho_i(r) \ln \frac{\rho_i(r)}{\rho_{i0}} - (\rho_i(r) - \rho_{i0})) dV$$

where ρ_{i0} is the density of the mobile charges in a reservoir connected to the system under investigation. Entropy by itself would clearly lead to a uniform distribution of counterions between the charged bodies, $\rho_i(r) = \rho_{i0}$, while together with the electrostatic energy it obviously leads to a nonmonotonic profile of the mobile charge distribution between the surfaces, minimizing the total free energy of the mobile ions.

The above discussion, though being far from rigorous, contains all the important theoretical underpinnings known

as the Poisson-Boltzmann theory (27). In order to arrive at the central equation corresponding to the core of this theory, one simply has to formally minimize the free energy, $F = W - TS$, together with the basic electrostatic equation (28) (Poisson equation) connecting the sources of the electrostatic field with the charge densities of different ionic species,

$$\epsilon \epsilon_0 \operatorname{div} E(r) = \sum_i e_i \rho_i(r)$$

where e_i is the charge on the mobile charged species i . The standard procedure now is to minimize the free energy, take into account the Poisson equation, and what follows is the well-known Poisson-Boltzmann equation, the solution of which gives the nonuniform profile of the mobile charges between the surfaces with fixed charges. This equation can be solved explicitly for some particularly simple geometries (27). For two charged planar surfaces the solution gives a screened electrostatic potential that decays exponentially away from the walls. It is thus smallest in the middle of the region between the surfaces and largest at the surfaces. The characteristic length of this decay, the Debye length,

$$\lambda_D = \sqrt{\frac{\epsilon \epsilon_0 kT}{\sum_i e_i^2 \rho_{i0}}}$$

away from the surfaces is independent of the surface charge. For uni-uni valent salts, the Debye screening length is numerically close to $3 \text{ \AA} / \sqrt{I}$, where I is the ionic strength of the salt in moles per liter. The exponential decay of the electrostatic field away from the charged surfaces with a characteristic length independent (to the lowest order) of the surface charge is one of the most important results of the Poisson-Boltzmann theory.

Obviously as the surfaces come closer together, their decaying electrostatic potentials begin to interpenetrate (25). The consequence of this interpenetration is a repulsive force between the surfaces that again decays exponentially with the intersurface separation and a characteristic length again equal to the Debye length. For two planar surfaces at a separation, D , bearing sufficiently small charges, characterized by the surface charge density, σ , so that the ensuing electrostatic potential is never larger than kT/e , one can derive (27) for the interaction free energy per unit surface area, $F(D)$, the expression

$$F(D) = \frac{\sigma^2 \lambda_D}{\epsilon \epsilon_0} (\coth(D/\lambda_D) - 1)$$

The typical magnitude of the electrostatic interaction in different systems of course depends on the magnitude of

the surface charge. It would not be unusual in lipids to have surface charge densities in the range of one unit charge per 50–100 Å² (29).

The same type of analysis would also apply to two charged cylindrical bodies, e.g., two molecules of DNA, interacting across an electrolyte solution. What one evaluates in this case is the interaction free energy per unit length of the cylinders (30), $g(R)$, that can be obtained in the form

$$g(R) = \frac{\mu^2}{2\pi\epsilon\epsilon_0} K_0(R/\lambda_D)$$

where $K_0(x)$ is the modified cylindrical Bessel function that has an asymptotic form of $K_0(x) \sim (1/\sqrt{x}) \exp(-x)$. It is actually possible to get an explicit form (30) of the interaction energy between two cylinders even if they are skewed by an angle, θ , between them. In this case the relevant quantity is the interaction free energy itself (if θ is nonzero, then the interaction energy does not scale with the length of the molecules) that can be obtained in a closed form as

$$F(R, \theta) = \frac{\mu^2 \lambda_D}{2\pi\epsilon\epsilon_0} \sqrt{\frac{2\pi R}{\lambda_D}} \frac{e^{-R/\lambda_D}}{\sin \theta}$$

The predictions for the forces between charged colloid bodies have been reasonably well borne out for electrolyte solutions of uni-uni valent salts (31). In that case there is near quantitative agreement between theory and experiment. However, for higher valency salts the Poisson-Boltzmann theory not only gives the wrong numerical values for the strength of the electrostatic interactions, but also misses their sign. In higher-valency salts the correlations among mobile charges between charged colloid bodies due to thermal fluctuations in their mean concentration lead effectively to attractive interactions (32), that are in many respect similar to van der Waals forces.

D. van der Waals Forces

van der Waals charge fluctuation forces are special in the sense that they are a consequence of thermodynamic as well as quantum mechanical fluctuations of the electromagnetic fields (15). They exist even if the average charge, dipole moment or higher multipole moments, on the colloid bodies are zero. This is in stark contrast to electrostatic forces that require a net charge or a net polarization to drive the interaction. This also signifies that the van der Waals forces are much more general and ubiquitous than any other force between colloid bodies (9).

There are many different approaches to van der Waals forces (33). For interacting molecules, one can distinguish

different contributions to the van der Waals force, stemming from thermally averaged dipole-dipole potentials (the Keesom interaction), dipole-induced dipole interactions (the Debye interaction), and induced dipole-induced dipole interactions (the London interaction) (34). They are all attractive, and their respective interaction energy decays as the sixth power of the separation between the interacting molecules. The magnitude of the interaction energy depends on the electromagnetic adsorption (dispersion) spectrum of interacting bodies, thus also the term dispersion forces.

For large colloidal bodies composed of many molecules, the calculation of the total van der Waals interaction is no trivial matter (15), even if we know the interactions between individual molecules composing the bodies. Hamaker assumed that one can simply add the interactions between composing molecules in a pairwise manner. It turned out that this was a very crude and simplistic approach to van der Waals forces in colloidal systems, as it does not take into account the highly nonlinear nature of the van der Waals interactions in condensed media. Molecules in a condensed body interact among themselves, thus changing their properties, which turn modify the van der Waals forces between them.

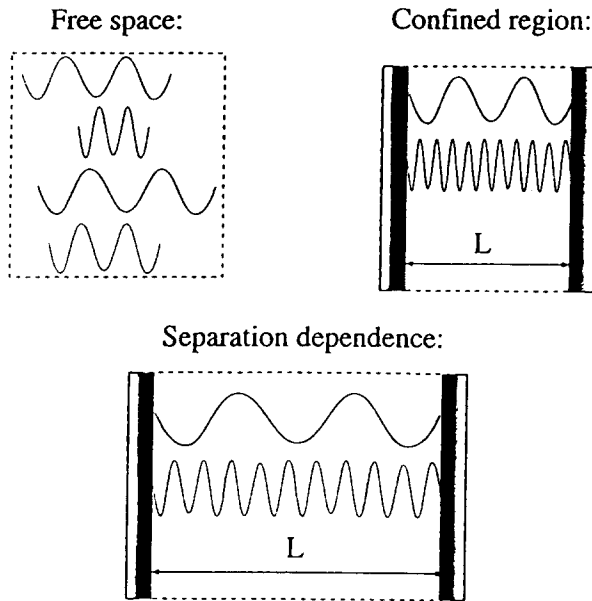
Lifshitz, following work of Casimir (9,15), realized how to circumvent this difficulty and formulated the theory of van der Waals forces in a way that already includes all these nonlinearities. The main assumption of this theory is that the presence of dielectric discontinuities as in colloid surfaces modifies the spectrum of electromagnetic field modes between these surfaces (Fig. 5). As the separation between colloid bodies varies, so do the eigenmode frequencies of the electromagnetic field between and within the colloid bodies. It is possible to deduce the change in the free energy of the electromagnetic modes due to the changes in the separation between colloid bodies coupled to their dispersion spectral characteristics (35).

From the work of Lifshitz it is now clear that if one associates the fluctuation free energy difference, F , with the change of the free energy of field harmonic oscillators at a particular eigenmode frequency, ω , as a function of the separation between the interacting bodies, D , and temperature, T ,

$$F = kT \ln \left(2 \sinh \frac{\hbar \omega(D)}{kT} \right) - kT \ln \left(2 \sinh \frac{\hbar \omega(\infty)}{kT} \right)$$

this change is nothing but the van der Waals interaction energy. With this equivalence in mind, it is quite straightforward to calculate the van der Waals interaction free energy between two planar surfaces at a separation, D , and temperature, T ; the dielectric constant between the two sur-

$$F_{vdw}(L) = \sum_{\omega_L} F(\omega_L) - \sum_{\omega_0} F(\omega_0)$$



$$F(\omega_L) = kT \ln \left(2 \sinh \frac{\hbar \omega_L}{kT} \right) \longrightarrow F(\omega_L) = \hbar \omega_L$$

Figure 5 A pictorial introduction to the theory of Lifshitz-van der Waals forces between colloid bodies. Empty space is alive with electromagnetic (EM) field modes that are excited by thermal as well as quantum mechanical fluctuations. Their frequency is unconstrained and follows the black body radiation law. Between dielectric bodies only those EM modes survive that can fit in a confined geometry. As the width of the space between the bodies changes, so do the allowed EM mode frequencies. Every mode can be treated as a separate harmonic oscillator, each contributing to the free energy of the system. Since this free energy depends on the frequency of the mode, which in turn depends on the separation between the bodies, the total free energy of the EM modes depends on the separation between the bodies. This is the Lifshitz-van der Waals force (15).

faces is ϵ , and within the surfaces ϵ' must be known as a function of the frequency of the electromagnetic field (35). This is a consequence that in general the dielectric media comprising the surfaces as well as the space between them are dispersive, meaning that their dielectric functions depend on frequency of the electromagnetic field, i.e., $\epsilon = \epsilon(\omega)$. With this in mind one can derive the interaction free energy per unit surface area of the interacting surfaces in the form

$$F(D) = \frac{A}{12\pi D^2}$$

where the s.c. Hamaker coefficient, A , has been introduced as shorthand for

$$A = \frac{3kT}{4} \left(\frac{\epsilon(0) - \epsilon'(0)}{\epsilon(0) + \epsilon'(0)} \right)^2 + \frac{3\hbar}{4\pi} \int_0^\infty d\xi \left(\frac{\epsilon(i\xi) - \epsilon'(i\xi)}{\epsilon(i\xi) + \epsilon'(i\xi)} \right)^2$$

The first term in the Hamaker constant is due to thermodynamic fluctuations, such as Brownian rotations of the dipoles of the molecules composing the media or the averaged dipole-induced dipole forces and depends on the static ($\omega = 0$) dielectric response of the interacting media, while the second term is purely quantum mechanical in nature (15). The imaginary argument of the dielectric constants is not that odd since $\epsilon(i\xi)$ is an even function of ξ , which makes $\epsilon(i\xi)$ also a purely real quantity (35).

In order to evaluate the magnitude of the van der Waals forces, one thus has to know the dielectric dispersion, $\epsilon(\omega)$, of all the media involved. This is no simple task and can be accomplished only for very few materials (34). Experiments seem to be a much more straightforward way to proceed. The values for the Hamaker constants of different materials interacting across water are between 0.3 and 2.0×10^{-20} J. Specifically for lipids, the Hamaker constants are quite close to theoretical expectations except for the phosphatidylethanolamines, which show much larger attractive interactions probably due to headgroup alignment (31). Evidence from direct measurements of attractive contact energies as well as direct force measurements suggest that van der Waals forces are more than adequate to provide attraction between bilayers for them to form multilamellar systems (36).

For cylinders the same type of argument applies, except that due to the geometry the calculations are a bit more tedious (37). Here the relevant quantity is not the free energy per unit area but the interaction free energy per unit length of the two cylinders of radius a , $g(R)$, considered to be parallel at a separation R . The calculation (38) leads to the following form:

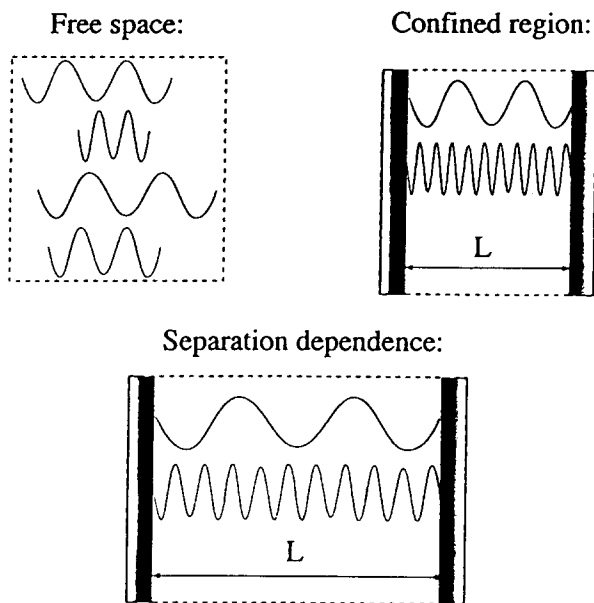
$$g(R) = \frac{3}{8} \frac{kT}{\pi} (\pi a^2) \left(\Delta_{\perp}^2 + \frac{1}{4} \Delta_{\perp} \Gamma + \Gamma^2 \frac{3}{2^7} \right) \frac{1}{R^5}$$

where

$$\Delta_{\parallel} = \frac{\epsilon_{\parallel} - \epsilon_m}{\epsilon_m} \Delta_{\perp} = \frac{\epsilon_{\perp} - \epsilon_m}{\epsilon_{\perp} + \epsilon_m}$$

with ϵ_{\parallel} the parallel and ϵ_{\perp} -the perpendicular components of the dielectric constant of the dielectric material of the

$$F_{\text{vdW}}(L) = \sum_{\omega_L} F(\omega_L) - \sum_{\omega_0} F(\omega_0)$$



$$F(\omega_L) = kT \ln \left(2 \sinh \frac{\hbar \omega_L}{kT} \right) \longrightarrow F(\omega_L) = \hbar \omega_L$$

Figure 5 A pictorial introduction to the theory of Lifshitz–van der Waals forces between colloid bodies. Empty space is alive with electromagnetic (EM) field modes that are excited by thermal as well as quantum mechanical fluctuations. Their frequency is unconstrained and follows the black body radiation law. Between dielectric bodies only those EM modes survive that can fit in a confined geometry. As the width of the space between the bodies changes, so do the allowed EM mode frequencies. Every mode can be treated as a separate harmonic oscillator, each contributing to the free energy of the system. Since this free energy depends on the frequency of the mode, which in turn depends on the separation between the bodies, the total free energy of the EM modes depends on the separation between the bodies. This is the Lifshitz–van der Waals force (15).

faces is ϵ , and within the surfaces ϵ' must be known as a function of the frequency of the electromagnetic field (35). This is a consequence that in general the dielectric media comprising the surfaces as well as the space between them are dispersive, meaning that their dielectric functions depend on frequency of the electromagnetic field, i.e., $\epsilon = \epsilon(\omega)$. With this in mind one can derive the interaction free energy per unit surface area of the interacting surfaces in the form

$$F(D) = \frac{A}{12\pi D^2}$$

where the s.c. Hamaker coefficient, A , has been introduced as shorthand for

$$A = \frac{3kT}{4} \left(\frac{\epsilon(0) - \epsilon'(0)}{\epsilon(0) + \epsilon'(0)} \right)^2 + \frac{3\hbar}{4\pi} \int_0^\infty d\zeta \left(\frac{\epsilon(i\zeta) - \epsilon'(i\zeta)}{\epsilon(i\zeta) + \epsilon'(i\zeta)} \right)^2$$

The first term in the Hamaker constant is due to thermodynamic fluctuations, such as Brownian rotations of the dipoles of the molecules composing the media or the averaged dipole–induced dipole forces and depends on the static ($\omega = 0$) dielectric response of the interacting media, while the second term is purely quantum mechanical in nature (15). The imaginary argument of the dielectric constants is not that odd since $\epsilon(i\zeta)$ is an even function of ζ , which makes $\epsilon(i\zeta)$ also a purely real quantity (35).

In order to evaluate the magnitude of the van der Waals forces, one thus has to know the dielectric dispersion, $\epsilon(\omega)$, of all the media involved. This is no simple task and can be accomplished only for very few materials (34). Experiments seem to be a much more straightforward way to proceed. The values for the Hamaker constants of different materials interacting across water are between 0.3 and 2.0×10^{-20} J. Specifically for lipids, the Hamaker constants are quite close to theoretical expectations except for the phosphatidylethanolamines, which show much larger attractive interactions probably due to headgroup alignment (31). Evidence from direct measurements of attractive contact energies as well as direct force measurements suggest that van der Waals forces are more than adequate to provide attraction between bilayers for them to form multilamellar systems (36).

For cylinders the same type of argument applies, except that due to the geometry the calculations are a bit more tedious (37). Here the relevant quantity is not the free energy per unit area but the interaction free energy per unit length of the two cylinders of radius a , $g(R)$, considered to be parallel at a separation R . The calculation (38) leads to the following form:

$$g(R) = \frac{3}{8} \frac{kT}{\pi} (\pi a^2) \left(\Delta_{\perp}^2 + \frac{1}{4} \Delta_{\perp} \Gamma + \Gamma^2 \frac{3}{27} \right) \frac{1}{R^3}$$

where

$$\Delta_{\parallel} = \frac{\epsilon_{\parallel} - \epsilon_m}{\epsilon_m} \quad \Delta_{\perp} = \frac{\epsilon_{\perp} - \epsilon_m}{\epsilon_{\perp} + \epsilon_m}$$

with ϵ_{\parallel} the parallel and ϵ_{\perp} the perpendicular components of the dielectric constant of the dielectric material of the

cylinders, while ϵ_m is the dielectric constant of the bathing medium. The above equation contains only the part of the van der Waals force corresponding to thermodynamic fluctuations. The corresponding quantum mechanical contribution is, however, easy to write down in complete analogy with the planar case.

If the two interacting cylinders are skewed at an angle θ , then the interaction free energy $G(R, \theta)$, this time not per length, is obtained (38) in the form

$$G(R, \theta) = -\frac{3 kT}{8 \pi} (\pi a^2)^2 \left(\Delta_{\perp}^2 + \frac{1}{4} \Delta_{\perp} \Gamma + \Gamma^2 \frac{2 \cos^2 \theta + 1}{2^7} \right) \frac{1}{R^4 \sin \theta}$$

The same correspondence between the thermodynamic and quantum mechanical parts of the interactions as for two parallel cylinders applies also to this case. Clearly the van der Waals force between two cylinders has a profound angular dependence that in general creates torque between the two interacting molecules.

Taking the numerical values of the dielectric constants for two interacting DNA molecules, one can calculate that the van der Waals forces are quite small, typically one to two orders of magnitude smaller than the electrostatic repulsions between them, and in general cannot hold the DNAs together in an ordered array. Other forces leading to condensation phenomena in DNA (10) clearly have to be added to the total force balance in order to get a stable array. There is as yet still no consensus on the exact nature of these additional attractions. It seems that they are due to the fluctuations of counterion atmosphere close to the molecules.

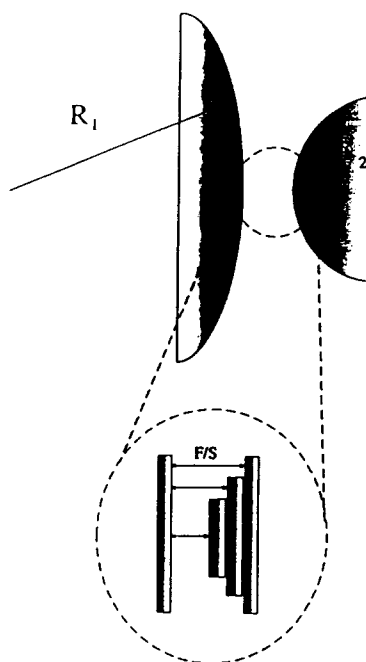
E. The DLVO Model

The popular Derjaguin-Landau-Verwey-Overbeek (DLVO) (9,25) model assumes that electrostatic double layer and van der Waals interactions govern colloid stability. Applied with a piety not anticipated by its founders, this model actually does work rather well in surprisingly many cases. Direct osmotic stress measurements of forces between lipid bilayers show that at separations less than $\sim 10 \text{ \AA}$ there are qualitative deviations from DLVO thinking (39). For μm -sized objects and for macromolecules at greater separations, electrostatic double-layer forces and sometimes van der Waals forces tell us what we need to know about interactions governing movement and packing.

F. Geometric Effects

Forces between macromolecular surfaces are most easily analyzed in plane-parallel geometry. Because most of the

interacting colloid surfaces are not planar, one has either to evaluate molecular interactions for each particular geometry or to devise a way to connect the forces between planar surfaces with forces between surfaces of a more general shape. The Derjaguin approximation (9) assumes that interactions between curved bodies can be decomposed into interactions between small plane-parallel sections of the curved bodies (Fig. 6). The total interaction between curved bodies would be thus equal to a sum where each term corresponds to a partial interaction between quasi plane-parallel sections of the two bodies. This idea can be given a completely rigorous form and leads to a connection between the interaction free energy per unit area of two interacting planar surfaces, $F(D)$, and the force acting between two spheres at minimal separation D , $f(D)$, one with the mean radius of curvature R_1 and the other



$$f(D) \approx 2\pi \left(\frac{R_1 R_2}{R_1 + R_2} \right) \frac{F(D)}{S}$$

Figure 6 The Derjaguin approximation. To formulate forces between oppositely curved bodies (e.g., cylinders, spheres) is very difficult. But it is often possible to use an approximate procedure. Two curved bodies (two spheres of unequal radii in this case) are approximated by a succession of planar sections, interactions between which can be calculated relatively easily. The total interaction between curved bodies is obtained through a summation over these planar sections.

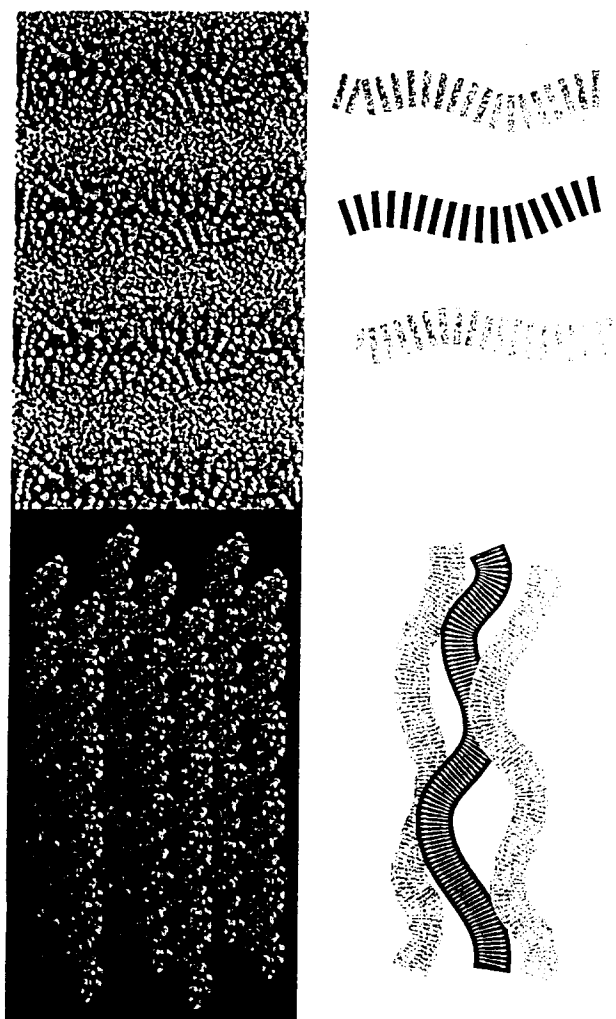


Figure 8 Thermally excited conformational fluctuations in a multilamellar membrane array or in a tightly packed polyelectrolyte chain array lead to collisions between membranes or polyelectrolyte chains. These collisions contribute an additional repulsive contribution to the total osmotic pressure in the array, a repulsion that depends on the average spacing between the fluctuating objects: $\langle D(x,y) \rangle$ for membranes and $\langle R(x,y) \rangle$ for polyelectrolyte chains. (The coordinates (x,y) point in the plane perpendicular to the average normal of the membrane, or perpendicular to the average direction of the polyelectrolyte chains.)

bodies bump into each other, which creates spikes of repulsive force between them. The average of this force is smooth and decays continuously with the mean separation between the bodies.

One can estimate this steric interaction for multilamellar lipid systems and for condensed arrays of cylindrical polymers. The only quantity entering this calculation is the

elastic energy, F_{el} , of a single bilayer, which can be written in the form

$$F_{el} = \frac{1}{2} K_c \int dS \left(\frac{1}{R_1} + \frac{1}{R_2} \right)^2$$

where K_c is the elastic modulus, usually between 10 and 50 kT (43) for different lipid membranes, dS is the element of surface area, and R_1 and R_2 are the two main curvatures of the membrane. If the instantaneous deviation of the membrane from its overall planar shape in the (x,y) plane is now introduced as $u(x,y)$, the presence of neighboring membranes introduces a constraint on the fluctuations of $u(x,y)$ that one can write as

$$\langle u(x,y)^2 \rangle = \text{const. } D^2$$

where D is the average separation between the membranes in a multilamellar stack. The free energy associated with this constraint can now be derived as (40).

$$F \propto \frac{(kT)^2}{K_c D^2}$$

It has obviously the same dependence on D as the van der Waals force. This is, however, not a general feature of undulation interactions as the next example clearly shows. Also, we only indicated the general proportionality of the interaction energy. Calculation of the prefactors can be difficult (44), especially because the elastic bodies usually do not interact with idealized hard repulsions but rather through soft potentials that have both attractive as well as repulsive regimes.

The same line of thought can now be applied to flexible polymers in a condensed array (42). This system is a one-dimensional analog of the multilamellar membrane system. For polymers the elastic energy can be written as

$$F_{el} = \frac{1}{2} K_c \int ds \left(\frac{1}{R} \right)^2$$

where again K_c is the elastic modulus, usually expressed through a persistence length $L_p = K_c/(kT)$, and ds is the element of the contour length along the polymer and R its local radius of curvature. Using the same constraint for the average fluctuations of the polymer away from the straight axis, one derives for the free energy change due to this constraint the relationship

$$F \propto \frac{kT}{L_p^{1/3} D^{2/3}}$$

Clearly the D dependence for this geometry is very much different from the one for van der Waals force, which would be D^{-5} . There is thus no general connection between the van der Waals force and the undulation fluctuation

one with R_2 . The formal equivalence can be written as follows:

$$f(D) = 2\pi \frac{R_1 R_2}{R_1 + R_2} F(D)$$

A similar equation can also be obtained for two cylinders in the form

$$f(D) = 2\pi \sqrt{R_1 R_2} F(D)$$

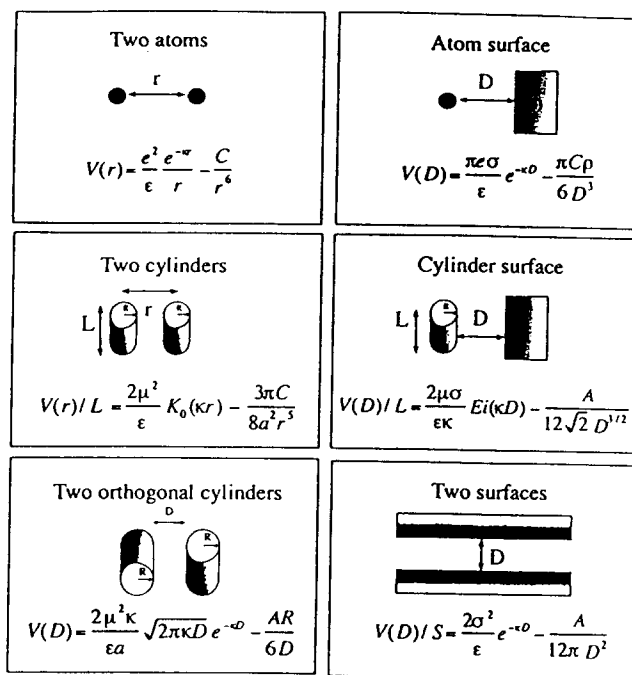
These approximate relations clearly make the problem of calculating interactions between bodies of general shape tractable. The only caveat here is that the radii of curvature should be much larger than the proximal separation between the two interacting bodies, effectively limiting the Derjaguin approximation to sufficiently small separations.

Using the Derjaguin formula or evaluating the interaction energy explicitly for those geometries for which this indeed is not an insurmountable task, one can now obtain a whole zoo of DLVO expressions for different interaction geometries (Fig. 7). The salient features of all these expressions are that the total interaction free energy always has a primary minimum, which can only be eliminated by strong short-range hydration forces, and a secondary minimum due to the compensation of screened electrostatic repulsion and van der Waals–Lifshitz attraction. The position of the secondary minimum depends as much on the parameters of the forces (Hamaker constant, fixed charges, and ionic strength) as well as on the interaction geometry. One can state generally that the range of interaction between the bodies of different shapes is inversely proportional to their radii of curvature.

Thus the longest-range forces are observed between planar bodies, and the shortest between small (point-like) bodies. What we have not indicated in Figure 7 is that the interaction energy between two cylindrical bodies, skewed at a general angle θ and not just for parallel or crossed configurations, can be obtained in an explicit form. It follows simply from these results that the configuration of two interacting rods with minimal interaction energy is the one corresponding to $\theta = \pi/2$, i.e., corresponding to crossed rods.

G. Fluctuation Forces

The term “fluctuation forces” is a bit misleading in this context because clearly van der Waals forces already are fluctuation forces. What we have in mind is thus a generalization of the van der Waals forces to situations where the fluctuating quantities are not electromagnetic fields but other quantities subject to thermal fluctuations. No general observation as to the sign of these interactions can be made; they can be either repulsive or attractive and are as a rule



Lowest order (linearized PB) separation dependence

Figure 7 A menagerie of DLVO interaction expressions for different geometries most commonly encountered in biological milieu: two small particles, a particle and a wall, two parallel cylinders, a cylinder close to a wall, two skewed cylinders, and two walls. The DLVO interaction free energy is always composed of a repulsive electrostatic part (calculated from a linearized Poisson-Boltzmann theory) and an attractive van der Waals part. μ = Charge per unit length of a cylinder; σ = charge per unit surface area of a wall; C = a geometry-dependent constant, ϵ = the dielectric constant, κ = the inverse Debye length, and ρ = the density of the wall material.

of thumb comparable in magnitude to the van der Waals forces.

The most important and ubiquitous force in this category is the undulation or Helfrich force (40). It has a very simple origin and operates among any type of deformable bodies as long as their curvature moduli are small enough (comparable to thermal energies). It was shown to be important for multilamellar lipid arrays (41) as well as in hexagonal polyelectrolyte arrays (42) (Fig. 8).

The mechanism is simple. The shape of deformable bodies fluctuates because of thermal agitation (Brownian motion) (26). If the bodies are close to each other the conformational fluctuations of one will be constrained by the fluctuations of its neighbors. Thermal motion makes the

force. Here again one has to indicate that if the interaction potential between fluctuating bodies is described by a soft potential, with no discernible hard core, the fluctuation interaction can have a profoundly different dependence on the mean separation (42).

Apart from the undulation fluctuation force, there are other fluctuation forces. The most important among them appears to be the monopolar charge fluctuation force (45), recently investigated in the context of DNA condensation. It arises from transient charge fluctuations along the DNA molecule due to constant statistical redistributions of the counterion atmosphere.

Although the theory of charge fluctuation forces is quite intricate and mathematically demanding (46), a simple argument will show the essential physics of it. Assume we have two point charges, e_1 and e_2 , at a separation, R , interacting through screened coulomb potential with a screening length again equal to the Debye length, λ_D , obtained by solving the linearized Poisson-Boltzmann equation. Together with the self-energies of the two charges, the total energy of the system can be written in the form

$$W(R) = \frac{e_1^2}{4\pi\epsilon_0\lambda_D} + \frac{e_2^2}{4\pi\epsilon_0\lambda_D} + \frac{e_1e_2}{4\pi\epsilon_0R}$$

If the two charges are not fixed, but are allowed to fluctuate, i.e., to explore all statistically available configurations, the partition function for the system, $\Xi(R)$, can be obtained from

$$\Xi(R) = \iint de_1 de_2 e^{-\beta W(R)}$$

where the integrals run over all values of the two fluctuating charges. Evaluating these two integrals by extending the range of integration to $(+\infty, -\infty)$, which introduces only a small error in the final result, we obtain to the lowest order in the separation between the two charges the result

$$F(R) = -kT \ln \Xi(R) = -kT \ln \left(1 + \left(\frac{\lambda_D}{R} \right)^2 e^{-2\kappa R} \right) \cong -kT \left(\frac{\lambda_D}{R} \right)^2 e^{-2\kappa R}$$

This simplified derivation already shows one of the salient features of the interaction potential for monopolar charge fluctuation forces, namely it is screened with half the Debye screening length. If there is no screening, however, the monopolar charge fluctuation force becomes the strongest and longest ranged among all the fluctuation forces. It is, however, much less general than the related van der Waals force, and at present it is still not clear what the detailed conditions should be for its appearance, the main difficulty being the question whether charge fluctua-

tions in the counterion atmosphere are constrained or not.

H. Lessons

Molecular forces apparently convey a variety that is surprising considering the fact that they are all to some extent or another just a variant of electrostatic interactions. Quantum and thermal fluctuations apparently modify the underlying electrostatics, leading to qualitatively novel and unexpected features. The zoo of forces obtained in this way is what one has to deal with and understand when trying to make them work for us.

III. DNA MESOPHASES

A. Polyelectrolyte Properties of DNA

We can define several levels of DNA organization similarly to Ref. 1. Its structure is the sequence of base pairs. Its secondary structure is the famous double helix that can exist in several conformations. In solution, the B-helical structure dominates (47). The bases are perpendicular to the axis of the molecule and are 0.34 nm apart, and 10 of them make one turn of the helix. These parameters can vary for DNA in solution, where up to 10.6 base pairs can make a whole turn of the double helix (48). In the A structure the bases are tilted with respect to the direction of the helix, and this arrangement yields an internal hole, wider diameter, and closer packing (Fig. 9). Other conformations, such as the left-handed Z form, are rare. In solution, DNA's tertiary structure includes the many bent and twisted conformations in three dimensions.

DNA lengths can reach macroscopic dimensions. For instance, the human genome is coded in approximately 3 billion base pairs with a collective linear stretch on the order of a meter. Obviously, this molecule must undergo extensive compaction in order to fit in the cell nucleus. In natural environments DNA is packaged by basic proteins, which form chromatin structures to keep DNA organized. In the test tube, DNA can be packaged into very tight and dense structures as well, primarily by various "condensing" agents. Their addition typically induces a random coil-to-globule transition. At large concentrations, DNA molecules, like lipids, form ordered liquid crystalline phases (10).

In vitro, at concentrations above a critical value (49), polyelectrolyte DNA self-organizes in highly ordered mesophases. In this respect it is lyotropic. But contrary to the case of lipid mesophases, where the shape of constituent molecules plays a determining role, the organization of DNA in condensed phases is primarily a consequence of

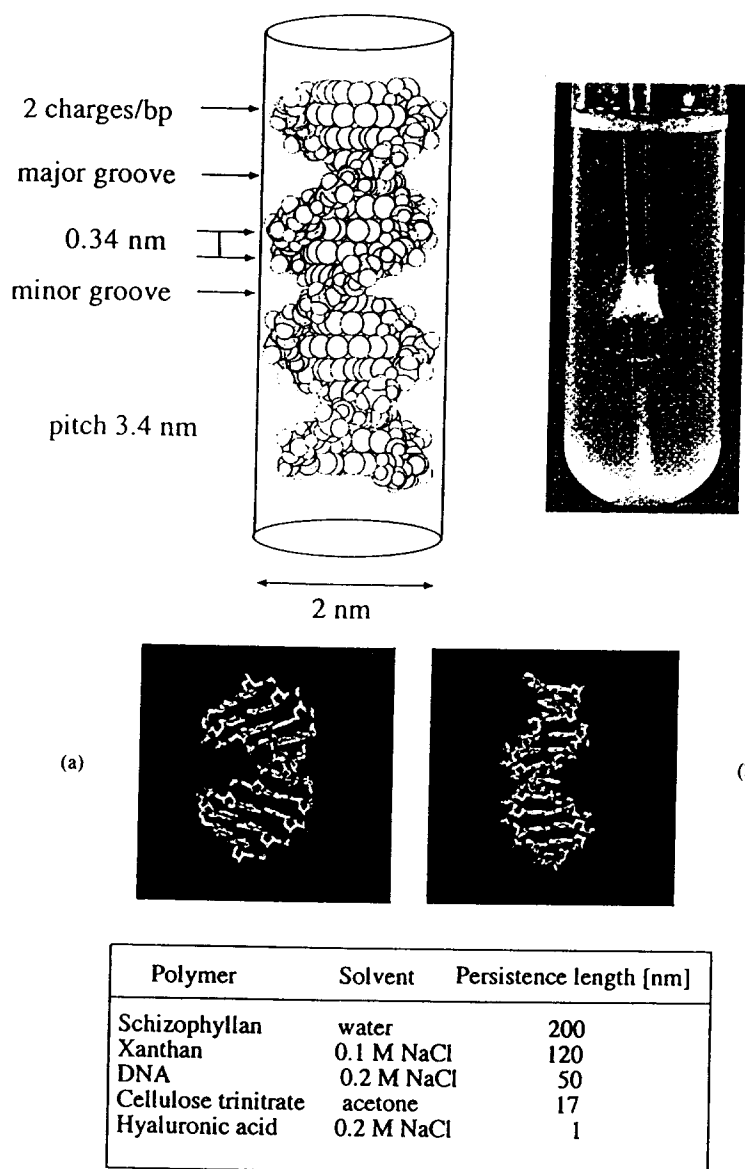


Figure 9 Structural parameters of a DNA molecule. The two relevant configurations of the DNA backbone: (a) A-DNA, common at small hydrations or high DNA densities, and (b) B-DNA, common in solution at large hydrations and lower DNA densities. The test tube holds ethanol precipitated DNA in solution. Its milky color is due to the light scattering by thermal conformational fluctuations in the hexatic phase (see main text). Table indicates typical persistence lengths for different (bio)polymer chains.

its relatively large stiffness (8). The orientational ordering of DNA at high concentrations is promoted mostly by the interplay between entropically favored disorder or misalignment and the consequent price in terms of the high interaction energy. The mechanism of orientational ordering is thus the same as in standard short nematogens (50), the main difference being due to the large length of poly-

meric chains. The discussion that follows will concentrate on very long—on the order of 1000 persistence lengths—DNA molecules.

B. Flexibility of DNA Molecules in Solution

In isotropic solutions, DNA can be in one of several forms. For linear DNA, individual molecules are effectively

straight over the span of a persistence length (defined as the exponential decay length for the loss of angular correlation between two positions along the molecule), while for longer lengths they form a worm-like random coil. The persistence length of DNA is about 500 (1). The persistence length has been determined by measuring the diffusion coefficient of different-length DNA molecules using dynamic light scattering and by enzymatic cyclization reactions (51). It depends only weakly on the base-pair sequence and ionic strength.

DNA can also be circular, as in the case of a plasmid. The closed form of a plasmid introduces an additional topological constraint on the conformation that is given by the linking number Lk (2). The linking number gives the number of helical turns along a circular DNA molecule. Because plasmid DNA is closed, Lk has to be an integer number. By convention, Lk of a closed right-handed DNA helix is positive. The most frequent DNA conformation for plasmids in cells is negatively supercoiled. This means that for such plasmids Lk is less than it would be for a torsionally relaxed DNA circle—negatively supercoiled DNA is underwound. This is a general phenomenon with important biological consequences. It seems that free energy of negative supercoiling catalyzes processes that depend on DNA untwisting, such as DNA replication and transcription, which rely on DNA (52). While the sequence of bases in exons determine the nature of proteins synthesized, it is possible that such structural features dictate the temporal and spatial evolution of DNA-encoded information.

C. Liquid Crystals

The fact that DNA is intrinsically stiff makes it form liquid crystals at high concentration (8). Known for about 100 years, the simplest liquid crystals are formed by rod-like molecules. Solutions of rods exhibit a transition from an isotropic phase with no preferential orientation to a nematic phase, a fluid in which the axes of all molecules point on average in one direction (Fig. 10). The unit vector in which the molecules point is called the nematic director, n . Nematic order is orientational order (50), in contrast to positional order that distinguishes between fluid and crystalline phases. Polymers with intrinsic stiffness can also form liquid crystals. This is because a long polymer with persistence length L_p acts much like a solution of individual rods that are all one persistence length long—polymer nematics (53).

If the molecules that comprise the liquid crystal are chiral, have a natural twist such as double-helical DNA, then their orientational order tends to twist. This twist originates from the interaction between two molecules that are both of the same handedness. This chiral interaction is illustrated

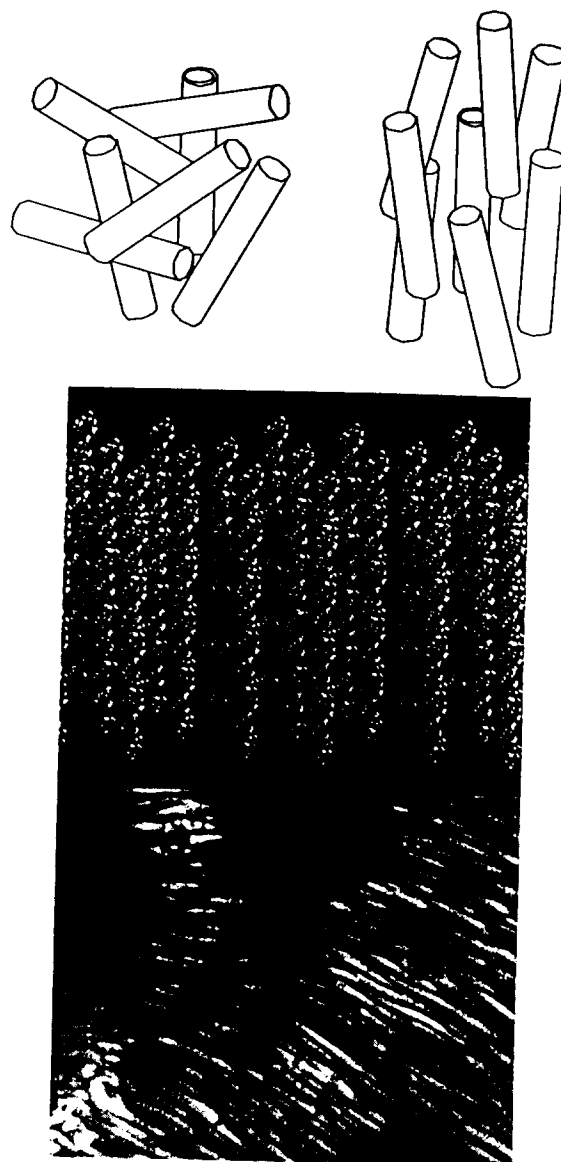


Figure 10 Nematic order in nondilute DNA solutions. The nematic state (50) is characterized by the average direction of the DNA molecules, here represented schematically by short cylinders. Locally DNAs are hexagonally packed with an average spacing that depends on applied osmotic pressure. Under crossed polarizers (bottom), the DNA nematic phase creates a characteristic striated texture. For long DNA molecules, the striations appear disordered.

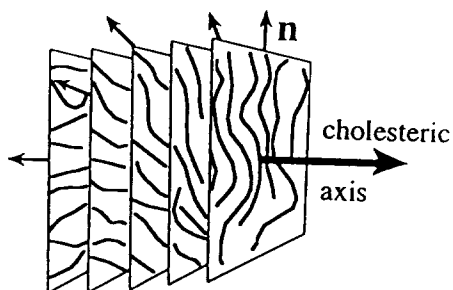
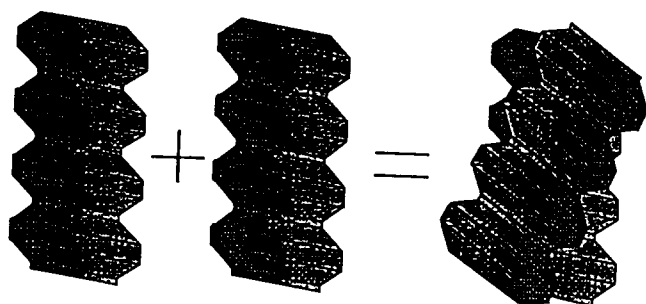


Figure 11 Chiral interaction for two helical or screw-like molecules. For steric reasons two helices pack best when slightly tilted with respect to each other. Instead of a nematic phase, chiral molecules form a cholesteric phase (50). The cholesteric phase is a twisted nematic phase in which the nematic director twists continuously around a cholesteric axis.

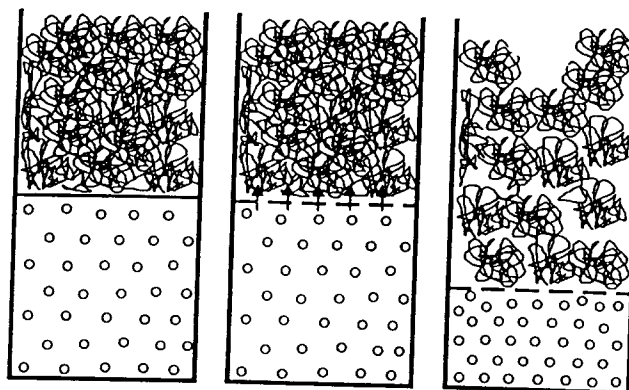
in Figure 11 for two helical or screw-like molecules. For steric reasons two helices pack best when tilted with respect to each other. Instead of a nematic phase, chiral molecules form a cholesteric phase (50). The cholesteric phase is a twisted nematic phase in which the nematic director twists continuously around the so-called cholesteric axis, as shown in Figure 11. Using the same arguments as for plain polymers, chiral polymers will form polymer cholesterics.

Both cholesteric and hexagonal liquid crystalline DNA phases were identified in the 1960s. This discovery was especially exciting because both phases were also found in biological systems. The hexagonal liquid crystalline phase can be seen in bacterial phages and the cholesteric phase seen in cell nuclei of dinoflagellates (8).

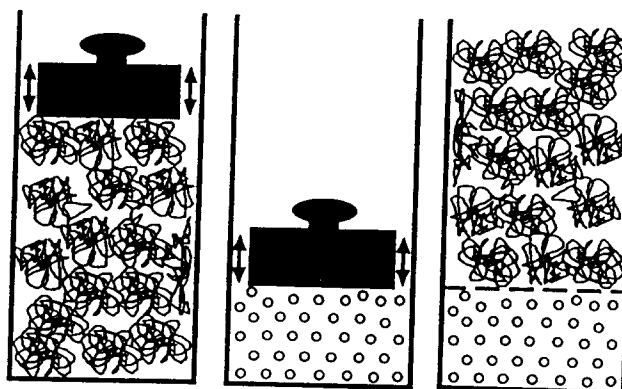
D. Measurements of Forces Between DNA Molecules

Liquid crystalline order lets us measure intermolecular forces directly. With the osmotic stress method, DNA liq-

uid crystals are equilibrated against neutral polymer (such as PEG or PVP) solutions of known osmotic pressure, pH, temperature, and ionic composition (54). Equilibration of DNA under osmotic stress of external polymer solution is effectively the same as exerting mechanical pressure on the DNA subphase with a piston (Fig. 12). In this respect the osmotic stress technique is formally very much similar



Equilibration of osmotic stress



Equivalence of osmotic stress

Figure 12 The osmotic stress method (18). DNA liquid crystals are equilibrated against solutions of a neutral polymer (such as PEG or PVP, depicted as disordered coils). These solutions are of known osmotic pressure, pH, temperature, and ionic composition (54). Equilibration of DNA under the osmotic stress of external polymer solution is effectively the same as exerting mechanical pressure on the DNA subphase with a piston that passes water and small solutes but not DNA. After equilibration under this known stress, DNA separation is measured either by x-ray scattering, if the DNA subphase is sufficiently ordered, or by densitometry (55). DNA density and osmotic stress thus determined immediately provide an equation of state (osmotic pressure as a function of the density of the DNA subphase) to be codified in analytic form over an entire phase diagram.

to the Boyle experiment, where one compresses a gas with mechanical pistons and measures the ensuing pressure. After equilibration under this known stress, DNA separation is measured either by x-ray scattering, if the DNA subphase is sufficiently ordered, or by straightforward densitometry (55). Known DNA density and osmotic stress immediately provide an equation of state (osmotic pressure as a function of the density of the DNA subphase) to be codified in analytic form for the entire phase diagram. Then, with the local packing symmetry derived from x-ray scattering (7,54), and sometimes to correct for DNA motion (42), it is possible to extract the bare interaxial forces between molecules, which can be compared with theoretical predictions as developed in Chapter 2. *In vivo* observation of DNA liquid crystals (56) shows that the amount of stress needed for compaction and liquid crystalline ordering is the same as for DNA *in vitro*.

E. Interactions Between DNA Molecules

Performed on DNA in univalent salt solutions, direct force measurements reveal two types of purely repulsive interactions between DNA double helices (4):

1. At interaxial separations less than ~ 3 nm (surface separation ~ 1 nm) an exponentially varying "hydration" repulsion is thought to originate from partially ordered water near the DNA surface.
2. At surface separations greater than 1 nm, measured interactions reveal electrostatic double-layer repulsion presumably from negative phosphates along the DNA backbone.

Measurements give no evidence for a significant DNA-DNA attraction expected on theoretical grounds (57). Though charge fluctuation forces must certainly occur, they appear to be negligible at least for liquid crystal formation in monovalent ion solutions. At these larger separations, the double-layer repulsion often couples with configurational fluctuations to create exponentially decaying forces, whose decay length is significantly larger than the expected Debye screening length (42).

Bare short-range molecular interactions between DNA molecules appear to be insensitive to the amount of added salt. This has been taken as evidence that they are not electrostatic in origin. The term "hydration force" associates these forces with perturbations of the water structure around DNA surface (54). Alternatively, short-range repulsion has been viewed as a consequence of the electrostatic force specific to high DNA density and counterion concentration (58).

F. High-Density DNA Mesophases

Ordering of DNA can be induced by two alternative mechanisms. First, attractive interactions between different DNA segments can be enhanced by adding multivalent counterions thought to promote either counterion-correlation forces (59) or electrostatic (60) and hydration attraction (22). In these cases DNA aggregates spontaneously. Alternatively, one can add neutral crowding polymers to the bathing solution that phase separate from DNA and exert osmotic stress on the DNA subphase (61). In this case the segment repulsions in DNA are simply counteracted by the large externally applied osmotic pressure. DNA is forced in this case to condense under externally imposed constraints. This latter case is formally (but only formally) analogous to a Boyle gas pressure experiment but with osmotic pressure playing the role of ordinary pressure, the main difference being that ordinary pressure is set mechanically, while osmotic pressure has to be set through the chemical potential of water, which is in turn controlled by the amount of neutral crowding polymers (such as PEG, PVP, or dextran) in the bathing solution (55).

At very high DNA densities, where the osmotic pressure exceeds 160 atm, DNA can exist only in a (poly)crystalline state (62). Nearest neighbors in such an array are all oriented in parallel and show correlated (nucleotide) base stacking between neighboring duplexes (Fig. 13). This means that there is a long-range correlation in the positions of the backbone phosphates between different DNA molecules in the crystal. The local symmetry of the lattice is monoclinic. Because of the high osmotic pressure, DNA is actually forced to be in an A conformation characterized by a somewhat larger outer diameter as well as a somewhat smaller pitch than in the canonical B conformation (see Fig. 9), which persists at smaller densities. If the osmotic pressure of such a crystal is increased above 400 atm, the helix begins to crack and the sample loses structural homogeneity (62).

Lowering the osmotic pressure does not have a pronounced effect on the DNA crystal until it is down to ~ 160 atm. Then the crystal as a whole simultaneously expands while individual DNA molecules undergo an A-B conformational transition (see Fig. 13) (62). This phase transformation is thus first order and, besides being a conformational transition for single DNAs is connected with the melting of the base stacking as well as positional order of the helices in the lattice. The ensuing low-density mesophase, where DNA is in the B conformation, is therefore characterized by short-range base-stacking order, short-range two dimensional (2D) positional order, and long-range bond orientational order (Fig. 14) (63). This order is connected with the spatial direction of the nearest neigh-

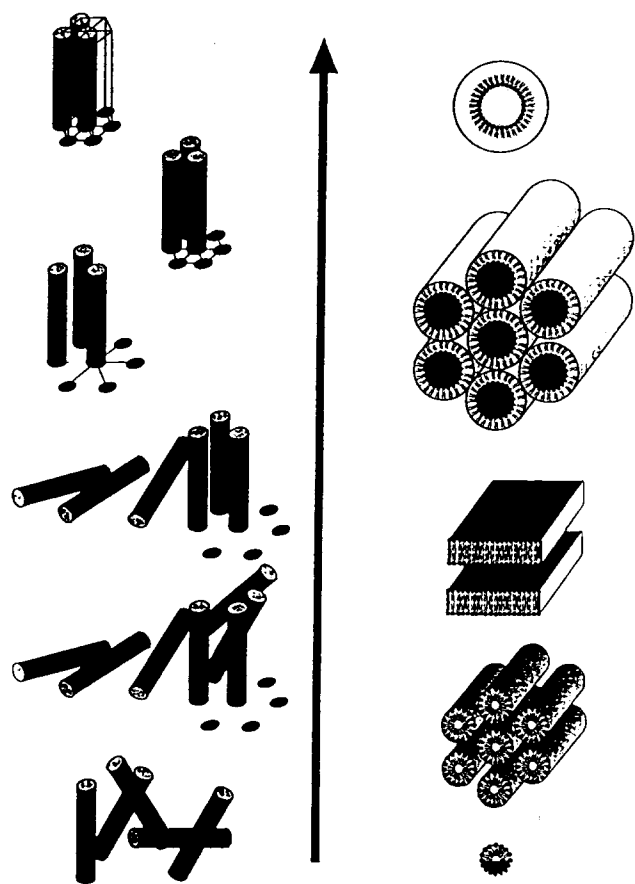


Figure 13 Schematic phase diagrams for DNA (left) and lipids (right). In both cases the arrow indicates increasing density in both cases. DNA starts (bottom) as a completely disordered solution. It progresses through a sequence of "blue" phases characterized by cholesteric pitch in two perpendicular directions (68), then to a cholesteric phase with pitch in only one direction. At still larger densities this second cholesteric phase is succeeded by a hexatic phase characterized by short-range liquid-like positional order and long-range crystal-like bond orientational or hexatic order (indicated by lines). At highest densities there is a crystalline phase, characterized by long-range positional order of the molecules and long-range base-stacking order in the direction of the long axes of the molecules. Between the hexatic and the crystalline forms, there might exist a hexagonal columnar liquid-crystalline phase that is similar to a crystal, but with base-stacking order only on short scales.

This lipid phase diagram (77) is a composite of results obtained for different lipids. It starts from a micellar solution and progresses through a phase of lipid tubes to a multilamellar phase of lipid bilayers. This is followed by an inverted hexagonal columnar phase of water cylinders and possibly goes to an inverted micellar phase. Most lipids show only a subset of these possibilities. Boundaries between the phases shown here might contain exotic cubic phases not included in this picture.

bors (64). It is for this reason that the phase has been termed a "line hexatic" phase. Hexatics usually occur only in 2D systems. They have crystalline bond orientational order but liquid-like positional order. There might be a hexatic-hexagonal columnar transition somewhere along the hexatic line, but direct experimental proof is lacking. The difference between the two phases is that the hexagonal columnar phase has also a crystalline positional order, a real 2D crystal (see Fig. 13) (65). It is the long-range bond orientational order that gives the line hexatic phase some crystalline character (66). The DNA duplexes are still packed in parallel, while the local symmetry perpendicular to the long axes of the molecules is changed to hexagonal. The directions of the nearest neighbors persist through macroscopic dimensions (on the order of mm), while their positions tend to become disordered after several (typically 5–10) lattice spacings. This mesophase has a characteristic x-ray scattering fingerprint (see Fig. 14). If the x-ray beam is directed parallel to the long axis of the molecules, it will show a hexagonally symmetrical diffraction pattern of broad liquid-like peaks (67).

Typical lattice spacings in the line hexatic phase are between 20 and 35 Å (i.e., between 600 and 300 mg/mL of DNA) (63). The free energy in this mesophase is mostly a consequence of the large hydration forces stemming from removal of water from the phosphates of the DNA backbone. Typically independent of the ionic strength of the bathing solution, these hydration forces (54) depend exponentially on the interhelical separation and decay with a decay length of about 3 Å (11) at these large densities.

When the osmotic pressure is lowered to about 10 atm (corresponding to interaxial spacing of about 35 Å, or DNA density of about 300 mg/mL), the characteristic hexagonal x-ray diffraction fingerprint of the line hexatic mesophase disappears continuously. This disappearance suggests the presence of a continuous, second-order transition into a low-density cholesteric (63). It is characterized by short-range (or effectively no) base-stacking order, short-range positional order, short-range bond orientational order, but long-range cholesteric order, manifested in a continuing rotation of the long axis of the molecules in a preferred direction. In this sense the cholesteric DNA mesophase would retain the symmetry of a one dimensional (1D) crystal. X-ray diffraction pattern of the DNA in the cholesteric phase is isotropic and has the form of a ring. Crossed polarizers, however, reveal the existence of long-range cholesteric order just as in the case of short chiral molecules. The texture of small drops of DNA cholesteric phase (spherulites) under crossed polarizers (Fig. 15) reveals the intricacies of orientational packing of DNA, where its local orientation is set by a compromise between interaction forces and macroscopic geometry of a spherulite. It is thus only at these low densities that the chiral character of the DNA

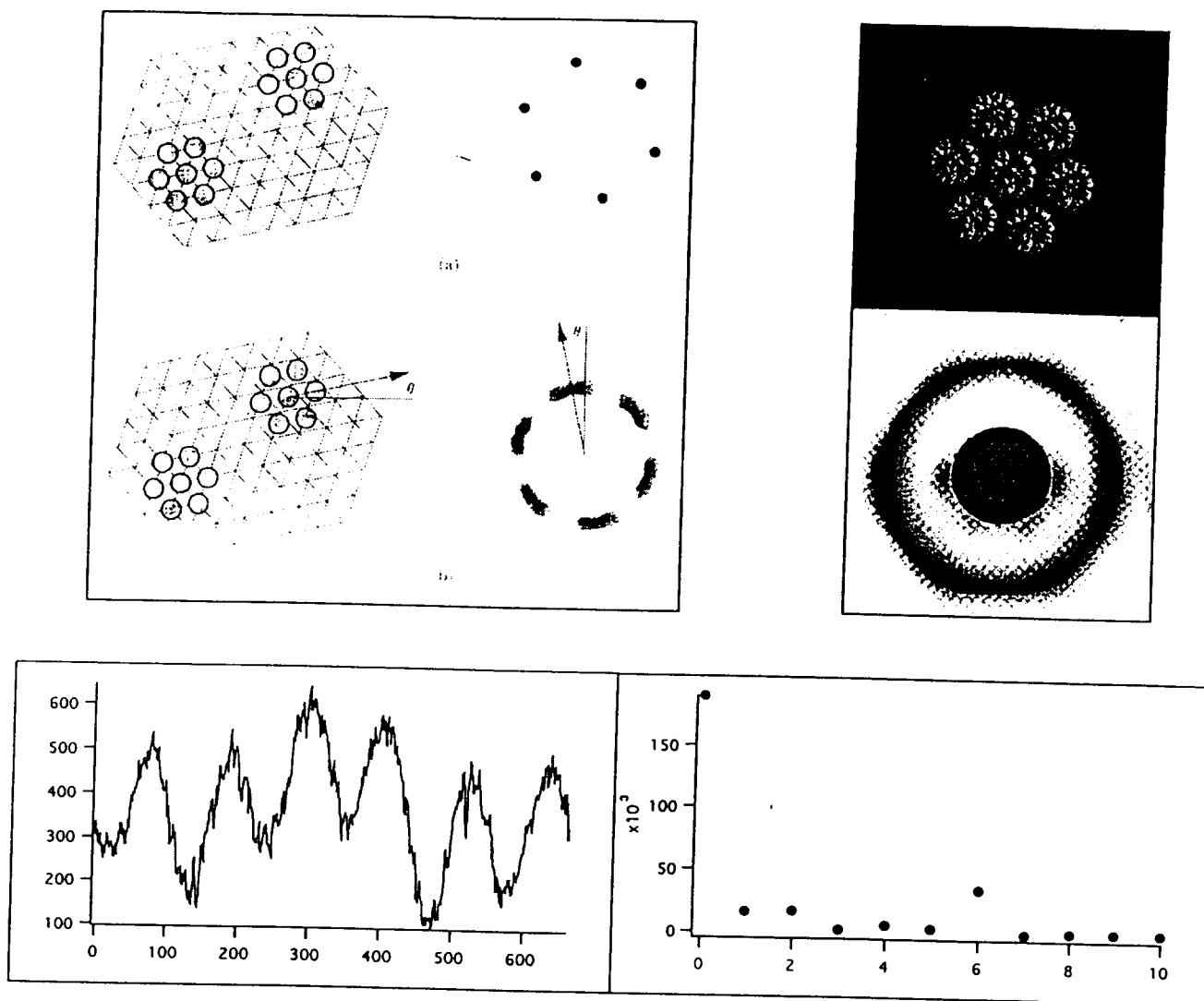


Figure 14 Bond orientational or hexatic order. With a real crystal, if one translates part of the crystal by a lattice vector, the new position of the atoms completely coincides with those already there. (Adapted from Ref. 67.) In a hexatic phase the directions to the nearest neighbors (bond orientations) coincide (after rotation by 60°), but the positions of the atoms don't coincide after displacement in one of the six directions! Consequently a real crystal gives a series of very sharp Bragg peaks in x-ray scattering (upper half of box), whereas a hexatic gives hexagonally positioned broad spots. The pattern of x-ray scattering by high-density DNA samples gives a fingerprint of a hexatic phase. The densitogram of the scattering intensity (right) shows six pronounced peaks that can be Fourier decomposed with a marked sixth order Fourier coefficient (left), another sign that the scattering is due to long-range bond orientational order (63).

finally makes an impact on the symmetry of the mesophase. It is not yet fully understood why the chiral order is effectively screened from the high-density DNA mesophases.

At still smaller DNA densities, the predominance of the chiral interactions in the behavior of the system remains. Recent work on the behavior of low-density DNA mesophases indicates (68) that the cholesteric part of the phase

diagram might end with a sequence of blue phases, which would emerge as a consequence of the loosened packing constraints coupled to the chiral character of the DNA molecule. At DNA density of about 10 mg/mL the cholesteric phase line would end with DNA reentering the isotropic liquid solution, where it remains at all subsequent densities, except perhaps at very small ionic strengths (69).

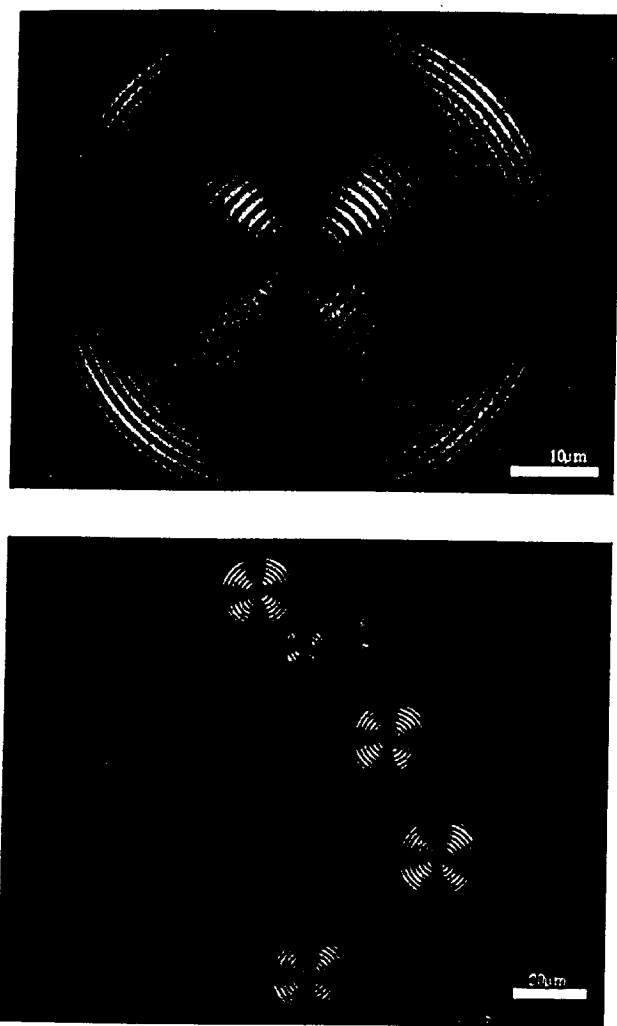


Figure 15 Texture of small drops of DNA cholesteric phase (spherulites) in a PEG solution under crossed polarizers at two different magnifications. These patterns reveal the intricacies of DNA orientational packing when its local orientation is set by a compromise between interaction forces and the macroscopic geometry of a spherulite. The change from a bright to a dark stripe indicates that the orientation of the DNA molecule has changed by 90 degrees.

G. DNA Equation of State

The free energy of the DNA cholesteric mesophase appears to be dominated by the large elastic shape fluctuations of its constituent DNA molecules (70), which leave their imprint in the very broad x-ray diffraction peak (55). Instead of showing the expected exponential decay characteristic of screened electrostatic interactions (71), where the decay length is equal to the Debye length, it shows a fluctuation-

enhanced repulsion similar to the Helfrich force existing in the flexible smectic multilamellar arrays (41). Fluctuations not only boost the magnitude of the existing screened electrostatic repulsion but also extend its range through a modified decay length equal to four times the Debye length. The factor-of-four enhancement in the range of the repulsive force is a consequence of the coupling between the bare electrostatic repulsions of exponential type and the elastic shape fluctuations described through elastic curvature energy that is proportional to the square of the second derivative of the local helix position (42). In the last instance it is a consequence of the fact that DNAs in the array interact via an extended, soft-screened electrostatic potential and not through hard bumps as assumed in the simple derivation in Chapter 2.

The similarity of the free energy behavior of the smectic arrays with repulsive interactions of Helfrich type and the DNA arrays in the cholesteric phase, which can as well be understood in the framework of the Helfrich-type enhanced repulsion, satisfies a consistency test for our understanding of flexible supermolecular arrays.

IV. LIPID MESOPHASES

A. Aggregation of Lipids in Aqueous Solutions

Single-molecule solutions of biological lipids exist only over a negligible range of concentrations; virtually all interesting lipid properties are those of aggregate mesophases such as bilayers and micelles. Lipid molecules cluster into ordered structures to maximize hydrophilic and minimize hydrophobic interactions (72,73). These interactions include negative free energy contribution from the solvation of polar heads and van der Waals interactions of hydrocarbon chains, competing with positive contributions such as steric, hydration, and electrostatic repulsions between polar heads. The "hydrophobic effect," which causes segregation of polar and nonpolar groups, is said to be driven by the increase of the entropy of the surrounding medium.

Intrinsic to the identity of surfactant lipids is the tension between water-soluble polar groups and lipid-soluble hydrocarbon chains. There is no surprise, then, that the amount of water available to an amphiphile is a parameter pertinent to its modes of packing and to its ability to incorporate foreign bodies.

These interactions, therefore, force lipid molecules to self-assemble into different ordered microscopic structures, such as bilayers, micelles (spherical, ellipsoidal, rod-like, or disk-like), which can, especially at higher concentrations, pack into macroscopically ordered phases, such as lamellar, hexagonal, inverted hexagonal, and cubic. The morphology of these macroscopic phases changes with the

balance between attractive van der Waals and ion correlation forces versus electrostatic, steric, hydration, and undulation repulsion (74).

B. The Lipid Bilayer

The workhorse of all lipid aggregates is the bilayer (Fig. 16) (73). This sandwich of two monolayers, with nonpolar hydrocarbon chains tucked in toward each other and polar groups facing water solution, is only about 20–30 Å thick.

Yet it has the physical resilience and the electrical resistance to form the plasma membrane that divides “in” from “out” in all biological cells. Its mechanical properties have been measured in terms of bending and stretching moduli. These strengths together with measured interactions between bilayers in multilamellar stacks have taught us to think quantitatively about the ways in which bilayers are formed and maintain their remarkable stability.

With some lipids, such as double-chain phospholipids, when there is the need to encompass hydrocarbon compo-

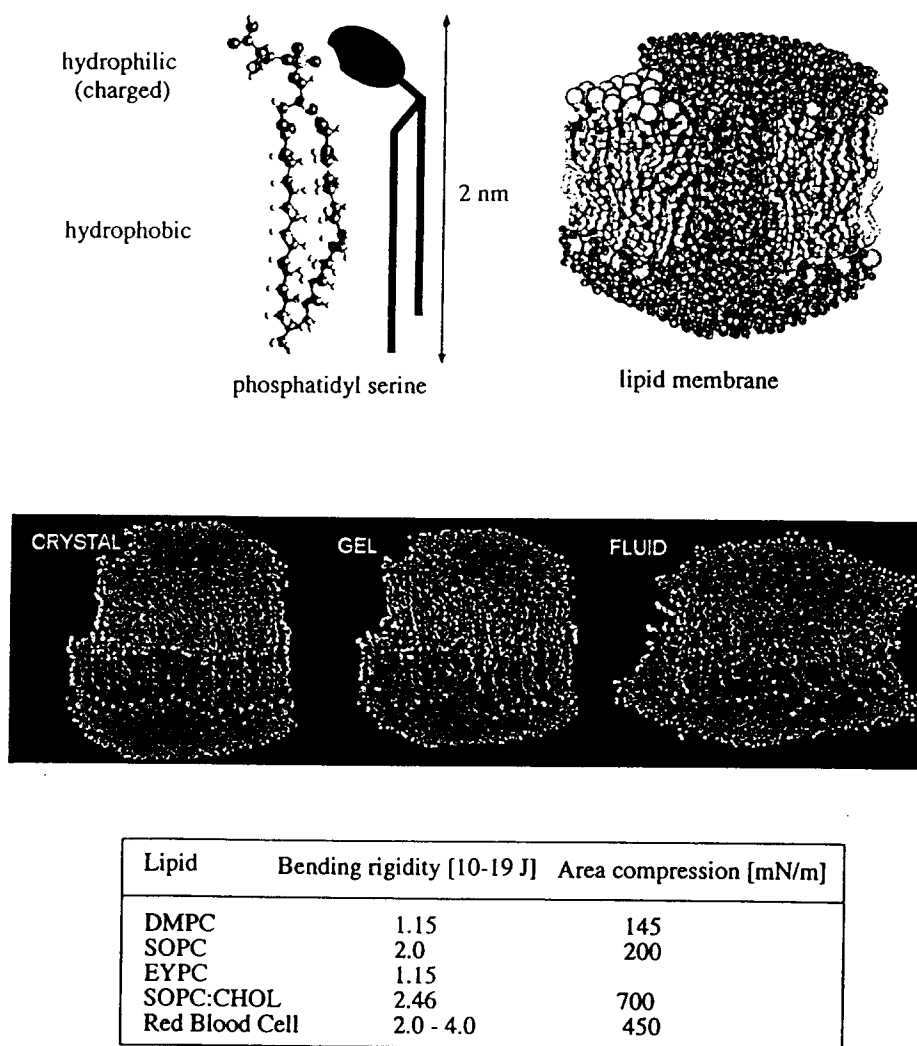


Figure 16 The lipid bilayer. A lipid molecule has a hydrophilic and a hydrophobic part (shown here is the phosphatidylserine molecule with a charged headgroup). At high enough densities lipid molecules assemble into a lipid bilayer. Together with membrane proteins, the lipid bilayer is the underlying structural component of biological membranes. The degree of order of the lipids in a bilayer depends drastically on temperature and goes through a sequence of phases (see main text): crystalline, gel, and fluid. The table at bottom gives sample values of bilayer bending rigidity and area compressibility for some biologically relevant lipids and one well-studied cell membrane. (Adapted from Ref. 110.)

nents voluminous compared with the size of polar groups, the small surface-to-volume ratio of spheres, ellipsoids, or even cylinders cannot suffice even at extreme dilution. Bilayers in this case are the aggregate form of choice. These may occur as single "unilamellar" vesicles, as onion-like multilayer vesicles, or multilamellar phases of indefinite extent. In vivo, bilayer-forming phospholipids create the flexible but tightly sealed plasma-membrane matrix that defines the inside from the outside of a cell. In vitro, multilayers are often chosen as a matrix of choice for the incorporation of polymers. Specifically, there are tight associations between positively charged lipids that merge with negatively charged DNA in a variety of forms (see below).

The organization of lipid molecules in the bilayer itself can vary (73). At low enough temperatures or dry enough conditions, the lipid tails are frozen in an all-*trans* conformation that minimizes the energy of molecular bonds in the alkyl tails of the lipids. Also, the positions of the lipid heads along the surface of the bilayer are frozen in 2D positional order, making the overall conformation of the lipids in the bilayer crystalline (L_C). The chains can be either oriented perpendicular to the bilayer surface (L_β and L_β') or tilted (crystalline phase L_C or ripple phase P_β). Such a crystalline bilayer cannot exist by itself, but assembles with others to make a real 3D crystal.

Upon heating, various rearrangements in the 2D crystalline bilayers occur; first the positional order of the headgroups melts leading to a loss of 2D order (L_β') and tilt (L_β), then at the gel-liquid crystal phase transition the untilted or rippled (P_β phase) bilayer changes into a bilayer membrane with disordered polar heads in two dimensions and conformationally frozen hydrocarbon chains, allowing them to spin around the long axes of the molecules, the so-called L_α phase. At still higher temperatures the thermal disorder finally destroys the ordered configuration of the alkyl chains, leading to a fluid-like bilayer phase. The fluid bilayer phase creates the fundamental matrix that according to the fluid mosaic model (72) contains different other ingredients of biological membranes, e.g., membrane proteins, channels.

Not only bilayers in multilamellar arrays but also liposome bilayers can also undergo such phase transition; electron microscopy has revealed fluid, rippled, and crystalline phases in which spherical liposomes transform into polyhedra due to very high values of bending elasticity of crystallized bilayers (75).

The fluid phase of the lipid bilayer is highly flexible. This flexibility makes it prone to pronounced thermal fluctuations, resulting in large excursions away from a planar shape. This flexibility of the bilayer is essential for understanding the zoo of equilibrium shapes that can arise in

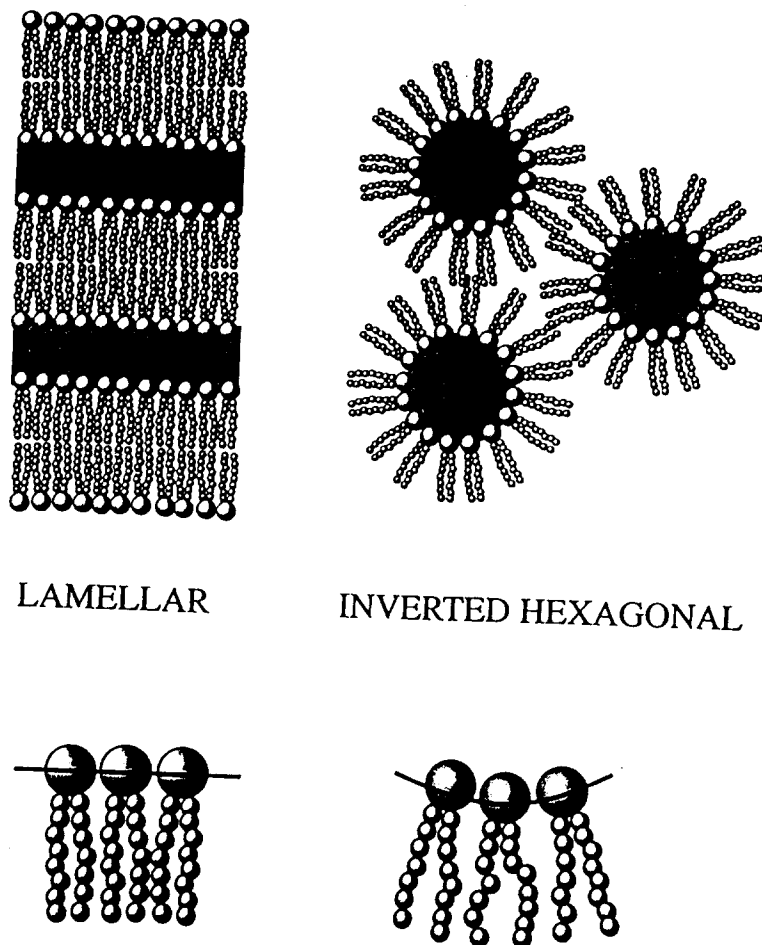
closed bilayer (vesicles) systems (76). Also, just as in the case of flexible DNA, it eventually leads to configurational entropic interactions between bilayers that have been crammed together (41). Bilayers and linear polyelectrolytes thus share a substantial amount of fundamentally similar physics, which allows us to analyze their behavior in the same framework.

C. Lipid Polymorphism

Low-temperature phases (77) are normally lamellar with frozen hydrocarbon chains, tilted (crystalline phase L_C or ripple phase P_β) or untilted (L_β and L_β' form 3, 2, or 1D crystalline or gel phases) with respect to the plane of the lipid bilayers. Terminology from thermotropic liquid crystal phenomenology (50) can be used efficiently in this context: these phases are smectic and SmA describes 2D fluid with no tilt while a variety of SmC phases with various indices encompass tilted phases with various degrees of 2D order. Upon melting, liquid crystalline phases with one- (lamellar L_α), two- (hexagonal II), or three-dimensional (cubic) positional order can form. The most frequently formed phases are micellar, lamellar, and hexagonal. Normal hexagonal phase consists of long cylindrical micelles ordered in a hexagonal array, while in the inverse hexagonal II phase water channels of inverse micelles are packed hexagonally with lipid tails filling the interstices. In excess water, such arrays are coated by a lipid monolayer. The morphology of these phases can be maintained upon their (mechanical) dispersal into colloidal dispersions. Despite the fact that energy has to be used to generate dispersed mesophases, relatively stable colloidal dispersions of particles with lamellar, hexagonal, or cubic symmetry can be formed.

Many phospholipids found in lamellar cell membranes after extraction, purification, and resuspension prefer an inverted hexagonal geometry (Fig. 13) (77). Under excess water conditions, different lipids will assume different most-favored spontaneous radii for the water cylinder of this inverted phase (78). An immediate implication is that different lipids are strained to different degrees when forced into lamellar packing. Lamellar-inverted hexagonal phase transitions occur with varied temperature, hydration, and salt concentration (for charged lipids), which form in order to alleviate this strain (Fig. 17).

In the presence of an immiscible organic phase, emulsion droplets can assemble (79). In regions of phase diagram, which are rich in water, oil-in-water emulsions and microemulsions can be formed, while in oil-rich regions these spherical particles have negative curvature and are therefore water-in-oil emulsions. The intermediate phase between the two is a bicontinuous emulsion that has zero



LAMELLAR

INVERTED HEXAGONAL

Figure 17 Different lipids are strained to different degrees when forced into lamellar packing. Relaxation of this strain contributes to the conditions for lamellar-to-inverted hexagonal phase transitions that depend on temperature, hydration, and salt concentration (for charged lipids). In the inverted hexagonal phase the lipid/aqueous solution interface is curved, thus relaxing the stresses developed in the tail region of the lipids.

average curvature and an anomalously low value of the surface tension (usually brought about the use of different cosurfactants) between the two immiscible components. Only microemulsions can form spontaneously (analogously to micelle formation), while for the formation of a homogeneous emulsion some energy has to be dissipated into the system.

The detailed structure of these phases as well as the size and shape of colloidal particles are probably dominated by (a) the average molecular geometry of lipid molecules, (b) their aqueous solubility and effective charge, (c) weaker interactions such as intra- and intermolecular hydrogen bonds, and (d) stereoisomerism as well as interactions within the medium. All of these depend on the temperature, lipid concentration, and electrostatic and van der Waals

interactions with the solvent and solutes. With charged lipids, counterions, especially anions, may also be important. Ionotropic transitions have been observed with negatively charged phospholipids in the presence of metal ions leading to aggregation and fusion (80). In cationic amphiphiles it was shown that simple exchange of counterions can induce micelle-vesicle transition. Lipid polymorphism is very rich, and even single-component lipid systems can form a variety of other phases, including ribbon-like phases, coexisting regions, and various stacks of micelles of different shapes.

D. Forces in Multilamellar Bilayer Arrays

Except for differences in dimensionality, forces between bilayers are remarkably similar to those between DNA.

At very great separations between lamellae, the sheet-like structures flex and "crumple" because of (thermal) Brownian motion (41). Just as an isolated flexible linear polymer can escape from its one linear dimension into the three dimensions of the volume in which it is bathed, so can two-dimensional flexible sheets. In the most dilute solution, biological phospholipids will typically form huge floppy closed vesicles; these vesicles enjoy flexibility while satisfying the need to keep all greasy nonpolar chains comfortably covered by polar groups rather than exposed at open edges. For this reason, in very dilute solution, the interactions between phospholipid bilayers are usually space wars of collision and volume occupation. This steric competition is always seen for neutral lipids; it is not always true for charged lipids (74).

Especially in the absence of any added salt, planar surfaces emit far-ranging electrostatic fields (27) that couple to thermally excited elastic excursions to create very long-range repulsion (44,83). As with DNA, this repulsion is a mixture of direct electrostatic forces and soft collisions mediated by electrostatic forces rather than by actual bilayer contact. In some cases electrostatic repulsion is strong enough to snuff out bilayer bending when bilayers form ordered arrays with periodicities as high as hundreds of Å (82).

Almost always bilayers align into well-formed stacks when their concentration approaches ~50–60 wt%, and their separation is brought down to a few tens of Å. In this region charged layers are quite orderly with little lamellar undulation. In fact, bilayers of many neutral phospholipids often spontaneously fall out of dilute suspension to form arrays with bilayer separations between 20 and 30 Å. These spontaneous spacings are thought to reflect a balance between van der Waals attraction and undulation-enhanced hydration repulsion (74). One way to test for the presence of van der Waals forces has been to add solutes such as ethylene glycol, glucose, or sucrose to the bathing solutions. It is possible then to correlate the changes in spacing with changes in van der Waals forces due to the changes in dielectric susceptibility through the relation as described above (83). More convincingly, there have been direct measurements of the work to pull apart bilayers that sit at spontaneously assumed spacings. This work of separation is of the magnitude expected for van der Waals attraction (84).

Similar to DNA, multilayers, of charged or neutral lipids, subjected to strong osmotic stress reveal exponential variation in force versus bilayer separation (74). Typically at separations between dry "contact" and 20 Å, exponential decay constants are 2–3 Å in distilled water or in salt solution, whether phospholipids are charged or neutral. Lipid bilayer repulsion in this range is thought to be due

to the work of polar group dehydration sometimes enhanced by lamellar collisions from thermal agitation (85). Normalized per area of interacting surface, the strength of hydration force acting in lamellar lipid arrays and DNA arrays is directly comparable.

Given excess water, neutral lipids will usually find the above-mentioned separation of 20–30 Å at which this hydration repulsion is balanced by van der Waals attraction. Charged lipids, unless placed in solutions of high salt concentration, will swell to take up indefinitely high amounts of water. Stiff charged bilayers will repel with exponentially varying electrostatic double-layer interactions, but most charged bilayers will undulate at separations where direct electrostatic repulsion has weakened. In that case, similar to what has been described for DNA, electrostatic repulsion is enhanced by thermal undulations (86).

E. Equation of State of Lipid Mesophases

Lipid polymorphism shows much less universality than DNA. This is, of course, expected since lipid molecules come in many different varieties (73) with strong idiosyncrasies in terms of the detailed nature of their phase diagrams. One thus can not achieve the same degree of generality and universality in the description of lipid phase diagram and consequent equations of state as was the case for DNA.

Nevertheless, recent extremely careful and detailed work on phosphatidylcholines (PCs) by J. Nagle and his group (87) points strongly to the conclusion that at least in the lamellar part of the phase diagram of neutral lipids, the main features of the DNA and lipid membrane assembly physics indeed is the same (85). This statement, however, demands qualification. The physics indeed is the same, provided one first disregards the dimensionality of the aggregates—one dimensional in the case of DNA and two dimensional in the case of lipid membranes—and takes into account the fact that while van der Waals forces in DNA arrays are negligible, they are essential in lipid membrane force equilibria. One of the reasons for this state of affairs is the large difference between the static dielectric constant of hydrophobic lipid tails and the aqueous solution bathing the aggregate.

We have already pointed out that in the case of DNA arrays, quantitative agreement between theory, based on hydration and electrostatic forces augmented by thermal undulation forces, and experiment has been obtained and extensively tested (7,42). The work on neutral lipids (85) claims that the same level of quantitative accuracy can be achieved in lipid membrane assemblies if one takes into account hydration and van der Waals forces, again augmented by thermal undulations. Of course the nature of the fluctuations in the two systems is different and is set by

the dimensionality of the fluctuating aggregates—one versus two dimensional.

The case of lipids adds an additional twist to the quantitative link between theory and experiments. DNA in the line hexatic as well as cholesteric phases (where reliable data for the equation of state exist) is essentially fluid as far as positional order is concerned and thus has unbounded positional fluctuations. Lipid membranes in the smectic multilamellar phase, on the other hand, are quite different in this respect. They are not really fluid as far as positional order is concerned but show something called quasi-long-range (QLR) order, meaning that they are in certain respects somewhere between a crystal and a fluid (50,67). The quasi-long-range positional order makes itself recognizable through the shape of the x-ray diffraction peaks in the form of persistent (Caille) tails (67). In a crystal one would ideally expect infinitely sharp peaks, broadened only because of finite accuracy of the experimental setup. Lipid multilamellar phases, however, show peaks with very broad and extended tails that are one of the consequences of QLR positional order. It is this property that allows us to measure not only the average spacing between the molecules but also the amount of fluctuation around this average spacing. Luckily the theory predicts that too, and without any free parameters (all of them being already determined from the equation of state) the comparison between predicted and measured magnitude in positional fluctuations of membranes in a multilamellar assembly is more than satisfactory (85).

In sum, the level of understanding of the equation of state reached for DNA and neutral lipid membrane arrays is pleasing.

V. DNA-CATIONIC LIPID COMPLEXES

A. The Nature of DNA-Lipid Interactions

DNA-lipid interactions retain all the characteristics of the DNA-DNA as well as lipid-lipid interactions described above. One obviously has hydration repulsion, electrostatic interaction, the sign of which depends on the sign of the lipid charges, as well as the ubiquitous van der Waals forces. The strengths of all these are well known. However, the tight binding of DNA to cationic lipid bilayers brings forth additional facets of the lipid DNA interactions, specific for this strong adsorption problem, that have not been addressed before.

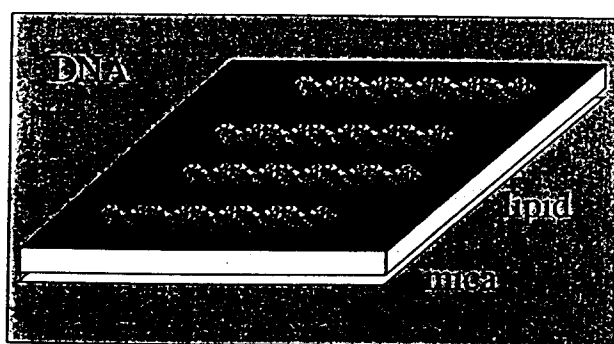
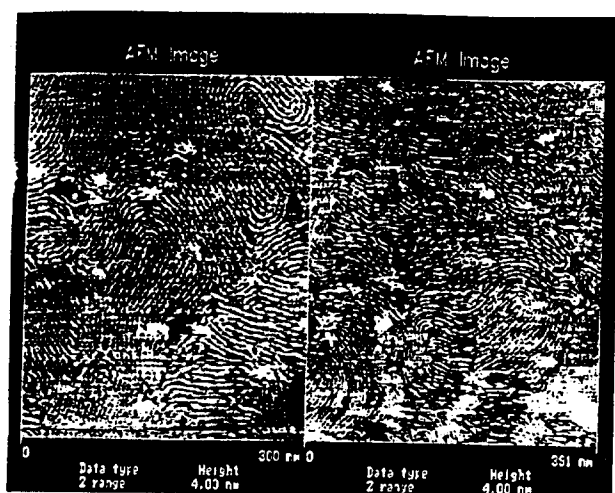
To understand the specifics of the DNA-cationic lipid interactions, consider first DNA adsorption to an isolated positively charged surface (88). We must compare free energies of free DNA plus that of bare surface with the free energy of the state in which the DNA is bound to the

surface. The driving force of adsorption comes from direct electrostatic attraction leading to charge neutralization as well as from the entropy increase of the counterions released from between the negative DNA and the positive surface. These counterions lower their electrostatic energy by accumulating near a charged body, but their translational entropy is reduced compared to that of ions far away (89). When DNA binds to a positively charged surface, counterions of both DNA and the surface are released into the bulk solution while DNA charge is neutralized by that of the positive surface. The net entropic change is the gain from released counterions minus the comparatively negligible conformational entropy loss of the bound DNA. The consequence of ion release is strongest when the surface charge density is high enough to neutralize all the charges on the DNA molecule.

DNA adsorbed to an immobilized surface still retains some flexibility in the plane of the surface and can thus interact with its neighbors through fluctuation interactions of the type that we already described in three-dimensional DNA assemblies. In the case of intercalation of DNA between the bilayers in a multilamellar lipid system, the fluctuations of DNA perpendicular to the planes of the bilayers are of course coupled to the membrane fluctuations themselves. Also there is the possibility that DNAs intercalated between different bilayers can still feel each other (90,91). All this adds to the difficulty in understanding the behavior of intercalated DNA.

B. Adsorption Studies of DNA

Experimentally, DNA adsorbed on cationic (DPTAB) as well as zwitterionic (DPPC) lipid bilayers was visualized using atomic force microscopy (AFM) as shown in Figure 18. DNA not only adsorbs to these surfaces but upon adsorption also condenses into nematically ordered two-dimensional structures. This two-dimensional ordering is characterized by a very low number of crossing defects (one DNA strand crossing another). Most DNAs remain in a locally parallel conformation throughout the sample. This is presumably an effect of the interplay between very strong (electrostatic neutralization) adsorption energies and the high stiffness of the DNA molecules. The average spacing between DNA molecules at zero added salt corresponds approximately to charge neutrality. Assuming an area per lipid of 70 \AA^2 and a DNA linear charge density of $1 e^-/1.7 \text{ \AA}$ suggests an average spacing of $76 \text{ \AA}^2/1.7 \text{ \AA} = 45 \text{ \AA}$ (vs. 43 \AA measured at zero salt). Similar experiments on varying charge densities that were prepared on a mixture of neutral and charged lipid showed that DNA slightly overcharges the surface (92). If the surface was initially



**DNA adsorbed on a lipid bilayer,
AFM imaging at 20 mM NaCl.**

Figure 18 DNA adsorbed onto a cationic lipid bilayer deposited onto a mica surface. An AFM image shows the strikingly ordered arrangement of the DNA on the surface. There are very few defects in patterns that spread over large domains. Changes in DNA-DNA separation as a function of the bathing solution ionic strength still elude explanation. (Courtesy J. Yang.)

positively charged, then after DNA adsorption it will be weakly negatively charged.

The exact equilibrium spacing between DNA molecules deposited on a cationic lipid surface also depends on the ionic strength of the bathing solution. Yang and Feng (93) measured this dependence for NaCl salt and obtained an increase in the separation between adsorbed DNA strands ranging from 43 Å in zero salt conditions and going all the way to almost 60 Å in 1 M salt. This dependence is in itself rather surprising because the addition of salt should screen the electrostatic interactions, leading consequently to smaller interaxial separations for larger ionic strengths.

Although there is no shortage of theories trying to come to grips with these perplexing results, no meaningful consensus has yet emerged. This remains one of the most surprising facts of DNA adsorption studies.

Also, by combining deposition of negative DNA layers with polycations (e.g., polyallylamine, polyethylenimine, polylysine, polyarginine) (94), one can create films with alternating negative and positive polyelectrolytes. Although the possible benefits of such complexes in DNA transfection studies are obvious, we shall not discuss them explicitly.

C. DNA-Lipid Complexes

When cationic lipid and DNA are mixed, complexes of different nature and symmetry can form (for a review see Ref. 95) and have indeed been observed in different studies. DNA-cationic liposome complexes were first examined under the electron microscope. Tight association of intact cationic liposomes and DNA was assumed in the early studies (96) without any unequivocal experimental proof. Electron microscopy and the inability of DNA to interact with intercalating agents was used by Gershon et al. (97) as proof that DNA-lipid interaction reorganizes the liposomes that eventually encapsulate DNA in their interior. Small added amounts of cationic lipid liposomes bind to DNA as beads-on-a-string. When more cationic lipids are added, DNA is completely encapsulated by a single lipid bilayer. At high liposome-to-DNA ratios, larger complexes form. Similar conclusions were also drawn by others (95). Later Sternberg et al. (98), basing their conclusion on freeze fracture electron microscopy, claimed that DNA is not only encapsulated within a liposome but is actually coated with a bilayer of cationic lipid. There were also claims that DNA could be hexagonally packed in the complex but unfortunately without any firm experimental evidence (99). All these structural models have only very indirect links to any direct structural probes that might unequivocally reveal the nature of the packing of DNA in the complexes.

D. Direct Structural Characterization of DNA-Lipid Complexes

The equilibrium DNA-cationic lipid phase diagram was investigated only recently by explicit structural small angle x-ray scattering studies. X-ray scattering probes local order in the DNA-lipid complex and allows one to deduce the symmetry of the packing, through analysis of the position of the diffraction peaks, as well as the range of the order, by studying the shape of each peak. In this respect it is of course the definitive method to study the structure of the complexes. X-ray scattering was first used as a probe to

characterize the nature of the DNA-lipid complex by Lasic et al. (100).

In this study DODAB-cholesterol liposomes were rapidly mixed with DNA, and the ensuing complexes were studied by x-ray scattering as well as cryomicroscopy. Both methods confirmed the structural model where DNA is intercalated between lipid bilayers (Fig. 19). X-ray diffraction revealed a succession of peaks that are a fingerprint of lamellar phase. The fundamental repeat distance was 64.4 Å. On this structure DNA scattering was superimposed as a separate peak corresponding to the interaxial separation of 36 Å (Fig. 20). Cryomicroscopy results were completely consistent, showing structures with fundamental periodicities of ~6.5 and 3.5 nm within particles of diameter below 0.5 μm. These *in vitro* results were later systematically studied by *in vivo* delivery studies of DNA-cationic lipid complexes (101). For these complexes, prepared with small liposomes, cryomicroscopy showed that complexes have a novel morphology and that DNA is condensed on the interior of invaginated liposomes between lipid bilayers. This structure is of course completely consistent with the intercalated DNA-lipid multilayers observed in *in vitro* studies.

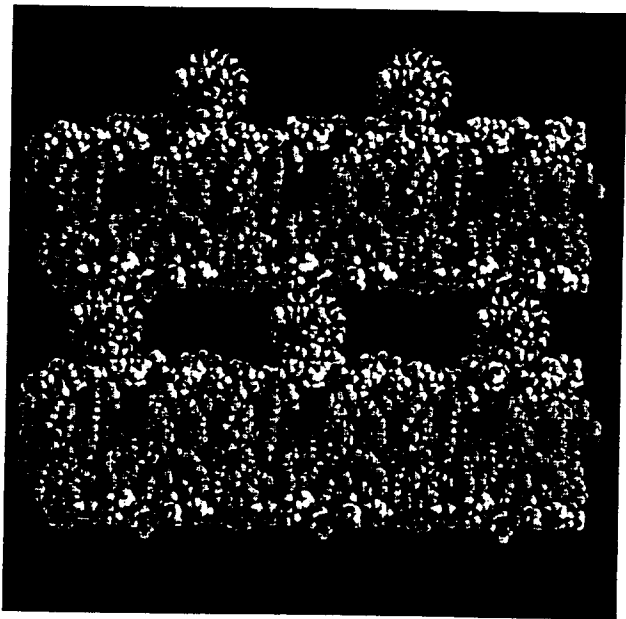


Figure 19 A model of DNA intercalated between cationic lipid bilayers. Cationic DODAB-cholesterol liposomes were rapidly mixed with DNA that intercalated between the cationic lipid membranes in the liposome. X-ray diffraction as well as cryomicroscopy confirmed that DNA is indeed intercalated between lipid bilayers. (Courtesy M. Hodošček.)

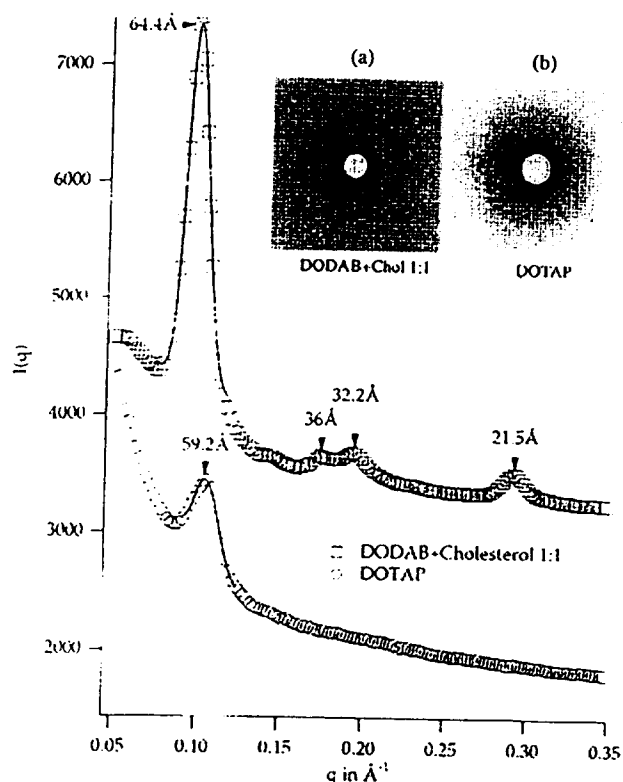


Figure 20 X-ray scattering from DODAB-cholesterol-DNA complexes. Three peaks (at 64.4, 32.2, and 21.5 Å) indicate the lamellar phase of the lipid subphase, whereas the peak at 36 Å corresponds to the intercalated DNA (see Fig. 19). The DNA peak also indicates that DNA between the lipid bilayers itself is at least partly ordered. The scattering pattern from cholesterol-free bilayers shows no intercalation of DNA.

X-ray diffraction studies on DNA lipid complexes were given further impetus by the beautiful work of Safinya and coworkers (102,103). They systematically studied the diffraction of DNA-cationic lipid complexes when one varies the charge on the lipid bilayers by changing the lipid:DNA ratio. A systematic variation in the spacing between intercalated DNA molecules was found that followed the amount of charge present in the lipid subphase (102). Also, detailed analysis of the form of the DNA diffraction peak revealed a very peculiar anisotropic nature of correlations between the DNA chains intercalated between different bilayers (104). Furthermore, it was shown that the intercalated lamellar phase of the DNA-cationic lipid complexes is not the only, and maybe even not the most relevant one in connection with transfection *in vivo*. Koltover et al. (103) realized that if DOPE or the cosurfactant hexanol are added to the cationic DOTAP lipid, the DNA-cationic lipid

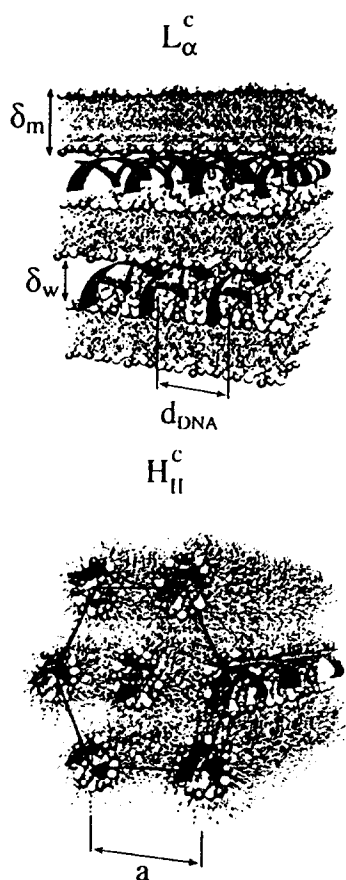


Figure 21 The structure of DNA-cationic lipid complexes in lamellar and inverted hexagonal phases. It seems that the lipids dictate the packing symmetry of the DNA-cationic lipid complex. While lipids can exist in both lamellar as well as inverted hexagonal phases (Fig. 13), lamellar packing of DNA by itself does not occur. These models of DNA packing in DNA-cationic lipid complexes demonstrate the power of x-ray scattering as a structural probe. (Adapted from Refs. 102, 103.)

shows the fingerprint of an inverted hexagonal phase (Fig. 21). In this phase, similarly to the hexagonal packing of DNA in concentrated solutions, DNA is arranged on the vertices of a hexagon, while lipids fill the space in between with their headgroups directed towards the charges on DNA. From the standpoint of the lipid this structure could also be called an inverted hexagonal phase, which is also well known for lipids in concentrated solutions. The way this transition comes about involves of course the two "helpers": DOPE and hexanol. DOPE is well known to make inverted hexagonal phases in solution because it is a conically shaped molecule that prefers strong negative curvatures. Hexanol, on the other hand, is a cosurfactant

that drastically diminishes the curvature modulus of the bilayer and thus allows it to wrap tightly around each DNA molecule.

The inverted hexagonal DNA-cationic lipid phase was found to be more efficient in transfection because it is less stable and readily fuses with membranes of anionic vesicles, thus releasing the trapped DNA (103). These results point strongly to a close connection between transfection efficiency and the structure of the DNA-cationic lipid complex. If this connection is further corroborated, there is hope that our knowledge regarding the polymorphism of DNA, lipids, and DNA-lipid complexes might prove essential in engineering the structure of DNA vectors that will yield a programmed release of DNA in transfection.

A detailed electrostatic calculation based on the ideas of the DLVO theory of colloid stability has been performed for both cases to give the free energy change upon complexation (105). Depending on surface charge density, complexation free energies are on the order of 6–10 kT/bp. Again, the driving force of complexation is due to the release of counterions into the bulk. If the link between transfection efficiency and the structure of the DNA-cationic lipid complexes withstands the test of time, theoretical estimates of the complexation energies are very important since they can provide much needed guidance in the search for appropriate formulations of successful transfection vehicles.

We might add at the end that the two DNA-cationic lipid complexes described above do not in any way exhaust all structural possibilities. The seminal work of Ghirlando (106) shows that one can expect a much richer structural phase diagram for DNA condensation induced by cationic surfactants, including lipids. The lamellar intercalated and inverted hexagonal phases might only be the tips of a much richer iceberg. One might also safely expect to find (107) structural phases where the lipid hexagonal phase, characterized by hexagonal columnar packing of cylindrical lipid micelles, will be intercalated with a DNA hexagonal columnar crystal (Fig. 22) or even cubic micellar phase intercalated with a cubic or hexagonal DNA packing. There is no way to say offhand whether these hypothetical structures might not introduce new twists into a rational theory of *in vivo* genome delivery.

E. Colloidal Properties of DNA-Lipid Complexes

To use DNA-cationic lipid complexes in nonviral gene therapy, the complexes must be small enough to escape from blood vessels and then to diffuse through tissue. At the same time these complexes have to be stable enough in

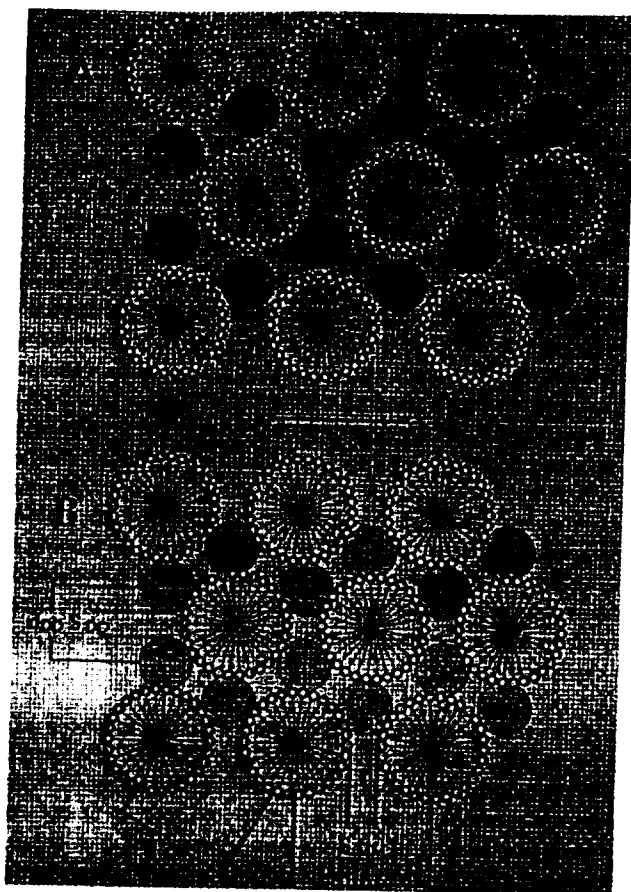


Figure 22 Lamellar and inverted hexagonal symmetries might not be the only possibilities for DNA–cationic lipid packing. Other structures of the DNA cationic surfactant assemblies have been seen. Here are two interpenetrating hexagonal lattices, one composed of DNA molecules and the other of cylindrical surfactant micelles at two different densities (A and B). (From Ref. 106, courtesy R. Ghirlando.)

serum to protect the DNA from nucleases and the immune system.

Colloidal properties of complexes can be determined by:

Capillary electrophoresis determining the electrostatic zeta-potential of the particles

Dynamic light scattering (DLS) for diffusion constants and consequently particle size

Single molecule counting devices that measure individual particle sizes from the flow of dilute suspensions through a small hole

Small size and solution stability can be achieved by preparing metastable overcharged complexes. Stable suspensions of complexes for *in vivo* transfection can be prepared by

extruding small vesicles from cationic lipid–helper lipid mixtures, which are then mixed with plasmid DNA (101). This procedure resulted in 100 nm complexes containing only few plasmid DNAs. Empirically, a ratio of 2 to 10 cationic charges per anionic DNA charge has been found to be optimal for efficient transfection. The excess positive charge inhibits aggregation into larger complexes. Even though larger complexes are thermodynamically more favorable, the electrostatic energy barrier between particles can be high enough to stabilize a suspensions of virus-size complexes for months. In most cases helper lipids like DOPE or cholesterol that mix with the cationic lipid improve efficiency. As discussed earlier, they do this most probably by being able to match better the surface charge density to the charge density on DNA.

Typically colloidal interactions are taken to be nonspecific. Using these concepts when dealing with a complex system like a cell requires caution. Most of a cell's interactions with its environmental are very specific. Therefore it is not surprising that endocytosis and transport to the nucleus depend more on the particular chemical composition than on the structure of the complexes. More studies of these specific mechanisms are needed to design better delivery systems.

VI. RETROSPECT AND PROSPECT

Structural elucidation of DNA–cationic lipid complexes and realization of the extent to which they share the structural features of pure DNA or pure lipid polymorphism have advanced notably in the past few years. Some old questions have been answered and new questions raised. It is these new questions that challenge our knowledge of the intricacies of interactions between macromolecules.

The DNA–lipid complexes found so far are only a sample of the much wider set of structures that will be seen on a full DNA–lipid phase diagram. We argue that this larger set of possibilities should be approached by firmly established methods to measure the energies of these structures at the same time that they are determined and located on a phase diagram. Built on principles of direct molecular interactions, recognizing the consequences of thermal agitation, this line of observation and analysis can lead to an understanding of the energetic whys and preparative hows of complex structures.

Forces so delineated are already knowledgeably applied in new preparations. Precisely how the structure of DNA–lipid aggregates will affect their efficacy in transfection remains to be seen. So far the ideas we have are too general and have been learned from studying analytically tractable but technically inadequate preparations. General principles do not lead to specific results. Molecules are too interesting to allow easy success in clinical design. Still,

there is little doubt of a practical link between the energy and structure of these complexes and their viability in a technological application.

Even the present general understanding of forces, even the cartoon ideas of the directions in which forces act in macromolecular complexes can tutor the bench scientist on how to improve preparations. There is enough known for a healthy iteration between experimental attempt and theoretical reason. Experimental successes and failures become the data for molecule force analyses. Various DNA-lipid assemblies reflect the various actions of competing forces. Molecular theorists can define and delineate these forces as they act to create each form; they can provide a logic to design variations in preparation. Basic scientists and clinicians are already in a position to help each other to improve their ways.

REFERENCES

- Bloomfield VA, Crothers DM, Tinoco I. *Nucleic Acids: Structures, Properties and Functions*. Mill Valley: University Science Books (Sausalito, CA), 1998.
- Vologotskii AV. *Topology and Physics of Circular DNA (Physical Approaches to DNA)*. Boca Raton: CRC Press, 1992.
- Strey HH, Podgornik R, Rau DC, Parsegian VA. *Colloidal DNA*. *Curr Op Coll Interf Sci* 1998; 3:534–539.
- Podgornik R, Strey HH, Parsegian VA. DNA-DNA Interactions. *Curr Op Struc Biol* 1998; 8:309–313.
- Kabanov VA, Flegner P, Seymour LW. *Self-Assembling Complexes for Gene Delivery*. New York: John Wiley and Sons, 1998.
- Lasic DD. *Liposomes in Gene Delivery*. Boca Raton, FL: CRC Press, 1997.
- Podgornik R, Rau DC, Parsegian VA. Parametrization of direct and soft steric-undulatory forces between DNA double helical polyelectrolytes in solutions of several different anions and cations. *Biophys J* 1994; 66:962–971.
- Livolant F, Leforestier A. DNA mesophases. A structural analysis in polarizing and electron microscopy. *Mol Cryst Liq Cryst* 1992; 215:47–56.
- Derjaguin BV, Churaev NV, Muller VM. *Surface Forces*. New York: Plenum Pub Corp, 1987.
- Bloomfield VA. DNA condensation. *Curr Op Struc Biol* 1996; 6:334–341.
- Leikin S, Parsegian VA, Rau DC, Rand RP. Hydration forces. *Annu Rev Phys Chem* 1993; 44:369–395.
- Darnell J, Lodish H, Baltimore D. *Molecular Cell Biology*. 2d ed. New York: Scientific American Books, 1990.
- Cerritelli ME, Cheng N, Rosenberg AH, McPherson CE, Booy FP, Steven AC. Encapsidated conformation of bacteriophage T7 DNA. *Cell* 1997; 91:271–280.
- Safinya CR, Koltover I, Rädler J. DNA at membrane surfaces: an experimental overview. *Curr Op Colloid Interf Sci* 1998; 1:69–77.
- Mahanty J, Ninham BW. *Dispersion Forces*. London: Academic Press, 1976.
- Safran SA. *Statistical Thermodynamics of Surfaces, Interfaces and Membranes*. New York: Addison Wesley, 1994.
- Eisenberg D, Kauzmann W. *The Structure and Properties of Water*. Oxford: Clarendon Press, 1969.
- Parsegian VA, Rand RP, Fuller NL, Rau DC. Osmotic stress for the direct measurement of intermolecular forces. *Methods Enzymol* 1986; 127:400–416.
- Marčelja S, Radić N. Repulsion of interfaces due to boundary water. *Chem Phys Lett* 1976; 42:129–130.
- Rand RP, Parsegian VA. Hydration forces between phospholipid bilayers. *Biochim Biophys Acta* 1989; 988:351–376.
- Kornyshev AA, Leikin S. Fluctuation theory of hydration forces: the dramatic effects of inhomogeneous boundary conditions. *Phys Rev A* 1998; 40:6431–6437.
- Rau DC, Parsegian VA. Direct measurement of the intermolecular forces between counterion-condensed DNA double helices. Evidence for long range attractive hydration forces. *Biophys J* 1992; 70:246–259.
- Parsegian VA. Long-range physical forces in the biological milieu. *Ann Rev Biophys Bioeng* 1973; 2:221–255.
- Bernal JD, Fankuchen I. X-ray and crystallographic studies of plant virus preparations. *J Gen Physiol* 1942; 25:111–165.
- Verwey EJW, Overbeek JTG. *Theory of the Stability of Lyophobic Colloids*. New York: Elsevier, 1948.
- Hill TL. *Statistical Mechanics. Principles and Selected Applications*. New York: Dover, 1956.
- Andelman D. Electrostatic properties of membranes: the Poisson-Boltzmann theory. In: Lipowsky R, Sackmann E, eds. *Structure and Dynamics of Membranes*. Vol. 1B. Amsterdam: Elsevier, 1995:603–642.
- Landau LD, Lifshitz EM. *The Classical Theory of Fields*. 4th ed. Oxford: Pergamon Press, 1986.
- McLaughlin S. Electrostatic potential at membrane solution interfaces. *Curr Top Membrane Transp* 1985; 4:71–144.
- Brenner SL, McQuarrie DA. Force balances in systems of cylindrical polyelectrolytes. *Biophys J* 1973; 13:301–331.
- Parsegian VA, Rand RP, Fuller NL. Direct osmotic stress measurements of hydration and electrostatic double-layer forces between bilayers of double-chained ammonium acetate surfactants. *J Phys Chem* 1991; 95:4777–4782.
- Kjellander R. Ion-ion correlations and effective charges in electrolyte and macroion systems. *Ber Bunsenges Phys Chem* 1996; 100:894–904.
- Hunter RJ. *Foundations of Colloid Science*. New York: Oxford University Press, 1987.
- Parsegian VA. Long range van der Waals forces. In: Olphen H, Mysels KL, eds. *Physical Chemistry: Enriching Topics from Colloid and Interface Science*. La Jolla: Theorex 1975:27–72.
- Landau LD, Lifshitz EM. *Statistical Physics Part 2*. Oxford: Pergamon Press, 1986.

36. Parsegian VA, Rand RP. Interaction in membrane assemblies. In: Lipowsky R, Sackmann E, eds. *Structure and Dynamics of Membranes*. Vol. 1B. Amsterdam: Elsevier, 1995:643–690.
37. Parsegian VA. Non-retarded van der Waals between anisotropic long thin rods at all angles. *J Chem Phys* 1972; 56: 4393–4397.
38. Brenner SL, Parsegian VA. A physical method for deriving the electrostatic interaction between rod-like polyanions at all mutual angles. *Biophys J* 1974; 14:327–334.
39. Parsegian VA, Fuller N, Rand RP. Measured work of deformation and repulsion of lecithin bilayers. *Proc Natl Acad Sci* 1979; 76:2750–2754.
40. Lipowsky R. Generic interactions of flexible membranes. In: Lipowsky R, Sackmann E, eds. *Structure and Dynamics of Membranes*. Vol. 1B. Amsterdam: Elsevier, 1995: 521–596.
41. Helfrich W. Steric interactions of fluid membranes in multilayer systems. *Z Naturforsch* 1978; 33a:305–315.
42. Strey HH, Parsegian VA, Podgornik R. Equation of state for polymer liquid crystals: theory and experiment. *Phys Rev E* 1998; 59:999–1008.
43. Seifert U, Lipowsky R. Morphology of Vesicles. In: Lipowsky R, Sackmann E, eds. *Structure and Dynamics of Membranes*. Vol. 1A. Amsterdam: Elsevier, 1995: 403–446.
44. Podgornik R, Parsegian VA. Thermal-mechanical fluctuations of fluid membranes in confined geometries: the case of soft confinement. *Langmuir* 1992; 8:557–562.
45. Podgornik R, Parsegian VA. Charge-fluctuation forces between rodlike polyelectrolytes: pairwise summability reexamined. *Phys Rev Lett* 1998; 80:1560–1563.
46. Ha BJ, Liu AJ. Counterion-mediated attraction between two like charged rods. *Phys Rev Lett* 1997; 79:1289–1292.
47. Saenger W. *Principles of Nucleic Acid Structure*. New York: Springer-Verlag, 1984.
48. Rhodes D, Klug A. Helical periodicity of DNA determined by enzyme digestion. *Nature* 1980; 286:573–578.
49. Rill RL. Liquid crystalline phases in concentrated DNA solutions. In: Pifa-Mrzljak G, ed. *Supramolecular Structure and Function*. New York: Springer, 1988:166–167.
50. De Gennes PG, Prost J. *The Physics of Liquid Crystals*. 2d ed. Oxford: Oxford University Press, 1993.
51. Hagerman PJ. Flexibility of DNA. *Ann Rev Biophys Biochem* 1988; 17:265–286.
52. Pruss GJ, Drlica K. DNA supercoiling and prokaryotic transcription. *Cell* 1989; 56:521–523.
53. Grosberg AY, Khokhlov AR. *Statistical Physics of Macromolecules (AIP Series in Polymers and Complex Materials)*. New York: American Institute of Physics, 1994.
54. Rau DC, Lee BK, Parsegian VA. Measurement of the repulsive force between polyelectrolyte molecules in ionic solution: hydration forces between parallel DNA double helices. *PNAS* 1984; 81:2621–2625.
55. Strey HH, Parsegian VA, Podgornik R. Equation of state for DNA liquid crystals: fluctuation enhanced electrostatic double layer repulsion. *Phys Rev Lett* 1997; 78: 895–898.
56. Reich Z, Wachtel EJ, Minsky A. In vivo quantitative characterization of intermolecular interaction. *J Biol Chem* 1995; 270:7045–7046.
57. Barrat JL, Joanny JF. Theory of polyelectrolyte solutions. In: Prigogine I, Rice SA, eds. *Advances in Chemical Physics*. New York: John Wiley and Sons, 1995:1–66.
58. Lyubartsev AP, Nordenskiöld L. Monte Carlo simulation study of ion distribution and osmotic pressure in hexagonally oriented DNA. *J Phys Chem* 1995; 99:10373–10382.
59. Oosawa F. *Polyelectrolytes*. New York: Marcel Dekker, 1971.
60. Rouzina I, Bloomfield VA. Macro-ion attraction due to electrostatic correlation between screening counterions. *J Phys Chem* 1996; 100:9977–9989.
61. Podgornik R, Strey HH, Rau DC, Parsegian VA. Watching molecules crowd: DNA double helices under osmotic stress. *Biophys Chem* 1995; 26:111–121.
62. Lindsay SM, Lee SA, Powell JW, Weidlich T, Demarco C, Lewen GD, Tao NJ, Rupprecht A. The origin of the A to B transition in DNA fibers and films. *Biopolymers* 1988; 17:1015–1043.
63. Podgornik R, Strey HH, Gawrisch K, Rau DC, Rupprecht A, Parsegian VA. Bond orientational order, molecular motion, and free energy of high-density DNA mesophases. *Proc Natl Acad Sci USA* 1996; 93:4261–4266.
64. Strandberg D. *Bond-Orientational Order in Condensed Matter Systems*. New York: Springer, 1992.
65. Durand D, Doucet J, Livolant F. A study of the structure of highly concentrated phases of DNA by x-ray diffraction. *J Phys II France* 1992; 2:1769–1783.
66. Kamien RD. Liquids with chiral bond order. *J Phys II France* 1996; 6:461–475.
67. Chaikin PM, Lubensky TC. *Principles of Condensed Matter Physics*. Cambridge: Cambridge University Press, 1995.
68. Leforestier A, Livolant F. DNA Liquid-crystalline blue phases—electron-microscopy evidence and biological implications. *Mol Cryst Liquid Cryst* 1994; 17:651–658.
69. Wang L, Bloomfield VA. Small-angle x-ray scattering of semidilute rodlike DNA solutions: polyelectrolyte behavior. *Macromolecules* 1991; 24:5791–5795.
70. Podgornik R, Rau DC, Parsegian VA. The action of interhelical forces on the organization of DNA double helices: fluctuation enhanced decay of electrostatic double layer and hydration forces. *Macromolecules* 1989; 22: 1780–1786.
71. Frank-Kamenetskii MD, Anshelevich VV, Lukashin AV. Polyelectrolyte model of DNA. *Sov Phys Usp* 1987; 4: 317–330.
72. Tanford C. *The Hydrophobic Effect. Formation of Micelles and Biological Membranes*. New York: John Wiley and Sons, 1980.
73. Cevc G, Marsh D. *Phospholipid Bilayers: Physical Principles and Models (Cell Biology: A Series of Monographs, Vol. 5)* New York: John Wiley & Sons.
74. Parsegian VA, Evans EA. Long and short range intermolecular and intercolloidal forces. *Curr Opin Coll Interf Sci* 1996; 1:53–60.
75. Duzgunes N, Wilshut L, Hong K, Fraley R, Perry C, Friends DS, James TL, Papahadjopoulos D. Physicochem-

- ical characterization of large unilamellar phospholipid vesicles prepared by reverse-phase evaporation. *Biochim. Biophys. ACTA* 1983; 732:289-299.
76. Seifert U. Configurations of fluid membranes and vesicles. *Adv Phys* 1997; 46:13-137.
 77. Small DM. *The Physical Chemistry of Lipids. From Alkanes to Phospholipids*. New York: Plenum Press, 1986.
 78. Gruner SM, Parsegian VA, Rand RP. Directly measured deformation energy of phospholipid H2 hexagonal phases. *Faraday Disc* 1986; 81:213-221.
 79. Daoud M, Williams CE. *Soft Matter Physics*. New York: Springer, 1999.
 80. Lasic DD. *Liposomes: From Physics to Applications*. Amsterdam: Elsevier, 1993.
 81. Parsegian VA, Podgornik R. Surface-tension suppression of lamellar swelling on solid substrates. *Colloids Surf A Physicochem Eng Asp* 1997; 129-130:345-364.
 82. Roux D, Safinya CR. A synchrotron x-ray study of competing undulation and electrostatic interlayer interactions in fluid multimembrane lyotropic phases. *J Phys-Paris* 1988; 49:307-318.
 83. Leneveu DM, Rand RP, Gingell D, Parsegian VA. Apparent modification of forces between lecithin bilayers. *Science* 1976; 191:399-400.
 84. Parsegian VA. Reconciliation of van der Waals force measurements between phosphatidylcholine bilayers in water and between bilayer coated mica surfaces. *Langmuir* 1993; 9:3625-3628.
 85. Gouliaev N, Nagle JF. Simulations of interacting membranes in soft confinement regime. *Phys Rev Lett* 1998; 81:2610-2613.
 86. Rand RP, Parsegian VA. Hydration forces between phospholipid bilayers. *Biochim Biophys Acta* 1989; 988: 351-376.
 87. Petrache HI, Gouliaev N, Tristram-Nagle S, Zhang R, Suter RM, Nagle JF. Interbilayer interactions from high-resolution x-ray scattering. *Phys Rev E* 1998; 57: 7014-7024.
 88. Fang Y, Yang J. Two-dimensional condensation of DNA molecules on cationic lipid membranes. *J Phys Chem* 1997; 101:441-449.
 89. Bruinsma R. Electrostatics of DNA-cationic lipid complexes: isoelectric instability. *Eur Phys J B* 1998; 4:75-88.
 90. O'Hern CS, Lubensky TC. Sliding columnar phase of DNA lipid complexes. *Phys Rev Lett* 1998; 80: 4345-4348.
 91. Golubovic L, Golubovic M. Fluctuations of quasi-two-dimensional smectics intercalated between membranes in multilamellar phases of DNA cationic lipid complexes. *Phys. Rev. Lett.* 1998; 80:4341-4344.
 92. Melghani MS, Yang J. Stable adsorption of DNA on zwitterionic lipid bilayers (preprint, 1999).
 93. Fang Y, Yang J. Two-dimensional condensation of DNA molecules on cationic lipid membranes. *J Phys Chem B* 1996; 101:441-449.
 94. Lvov Y, Decher G, Sukhorukhov G. Assembly of thin films by means of successive deposition of alternate layers of DNA and poly(allylamine). *Macromolecules* 1993; 26: 5396-5399.
 95. Lasic DD, Papahadjopoulos D, Podgornik R. Polymorphism of lipids, nucleic acids, and their interactions. In: Kabanov AV, Felgner PL, Seymour LW, eds. *Self-assembling complexes for gene delivery: from laboratory to delivery*. Chichester: J. Wiley, 1998:3-26.
 96. Felgner PL, Ringold GM. Cationic liposome-mediated transfection. *Nature* 1989; 337:387-388.
 97. Gershon H, Ghirlando R, Guttman SB, Minsky A. Mode of formation and structural features of DNA-cationic liposome complexes used for transfection. *Biochemistry* 1993; 32:7143-7151.
 98. Sternberg B, Sorgi FL, Huang L. New structures in complex-formation between DNA and cationic liposomes visualized by freeze-fracture electron-microscopy. *FEBS Lett* 1994; 356:361-366.
 99. Lasic DD, Barenholz Y. *Handbook of Nonmedical Applications of Liposomes: From Gene Delivery and Diagnostics to Ecology*. Boca Raton, FL: CRC Press, 1996:43-57.
 100. Lasic DD, Strey H, Stuart MCA, Podgornik R, Frederik PM. The structure of DNA-liposome complexes. *J Am Chem Soc* 1997; 119:832-833.
 101. Templeton NS, Lasic DD, Frederik PM, Strey HH, Roberts DD, Pavlakis GN. Improved DNA:liposome complexes for increased systemic delivery and gene expression. *Nature Biotechnol* 1997; 15:647-652.
 102. Radler JO, Koltover I, Salditt T, et al. Structure of DNA-cationic liposome complexes: DNA intercalation in multilamellar membranes in distinct interhelical packing regimes. *Science* 1997; 275:810-814.
 103. Koltover I, Salditt T, Radler JO, et al. An inverted hexagonal phase of cationic liposome-DNA complexes related to DNA release and delivery. *Science* 1998; 281:78-81.
 104. Salditt T, Koltover I, Radler O, et al. Self-assembled DNA-cationic-lipid complexes: two-dimensional smectic ordering, correlations, and interactions. *Phys Rev E* 1998; 58: 889-904.
 105. Harries D, May S, Gelbart WM, Ben-Shaul A. Structure, stability and thermodynamics of lamellar DNA-lipid complexes. *Biophys J* 1998; 75:159-173.
 106. Ghirlando R. DNA condensation induced by cationic surfactants. Ph.D. dissertation. The Weizmann Institute of Science, Rehovot, Israel, 1991.
 107. Ghirlando R. DNA Condensation induced by cationic surfactants. Ph.D. dissertation. The Weizmann Institute of Science, Rehovot, Israel, 1991.
 108. Kleinschmidt AK, Lang D, Jacherts D, Zahn RK. Darstellung und langen messungen des gesamten desoxyribonuclein-saure inhaltes von T2-bakteriophagen. *Biochim Biophys ACTA* 1962; 61:857-864.
 109. Kessel RG, Kardon RH. *Tissues and Organs*. San Francisco: W.H. Freeman and Co, 1979.
 110. Heller H, Schaefer M, Schulten K. Molecular dynamics simulation of a bilayer of 200 lipids in the gel and in the liquid-crystal phases. *J Phys Chem* 1993; 97:8343-8360.